ANNUAL RESEARCH REPORT

2020

Gary S. Was, Director
Ovidiu Toader, Manager and Lead Accelerator Scientist
Fabian Naab, Senior Accelerator Scientist
Thomas Kubley, Accelerator Scientist
Robert Hensley, Electronic Systems Engineer

2600 Draper Road
Department of Nuclear Engineering and Radiological Sciences
University of Michigan
Ann Arbor, Michigan 48109-2145
mibl.engin.umich.edu

Telephone: (734) 936-0131 Fax: (734) 763-4540

The Annual Research Report

This report summarizes the principal research activities in the Michigan Ion Beam Laboratory during the past calendar year. One hundred and twenty researchers conducted 48 projects at MIBL that accounted for 156 irradiations and 5910 hours of instrument usage. The programs included participation from researchers at the University, corporate research laboratories, private companies, government laboratories, and other universities across the United States. These projects also included 8 projects funded through the Nuclear Science User Facility program. The extent of participation of the laboratory in these programs ranged from routine surface analysis to triple beam irradiations. Experiments included Rutherford backscattering spectrometry, elastic recoil spectroscopy, nuclear reaction analysis, direct ion implantation, ion beam mixing, ion beam assisted deposition, and radiation damage by proton irradiation and self-ion irradiation, dual ion irradiation and triple beam irradiation. The following pages contain a synopsis of the research conducted in the Michigan Ion Beam Laboratory during the 2019 calendar year.

About the Laboratory

The Michigan Ion Beam Laboratory for Surface Modification and Analysis was completed in October of 1986. The laboratory was established for the purpose of advancing our understanding of ion-solid interactions by providing up-to-date equipment with unique and extensive facilities to support research at the cutting edge of science. Researchers from the University of Michigan as well as industry and other universities are encouraged to participate in this effort.

The lab houses a 3 MV Pelletron accelerator, a 1.7 MV tandem ion accelerator, and a 400 kV ion implanter that are configured to provide for a range of ion irradiation and ion beam analysis capabilities utilizing 9 beamlines, 5 target chambers and a transmission electron microscope. The control of the parameters and the operation of these systems are mostly done by computers and are interconnected through a local area network, allowing for complete control of irradiations from the control room as well as off-site monitoring and control.

In 2010, MIBL became a Partner Facility of the National Scientific User Facility (NSUF), based at Idaho National Laboratory, providing additional opportunities for researchers across the US to access the capabilities of the laboratory. In 2016, MIBL was recognized as the top ion beam laboratory in the U.S. by the Nuclear Science User Facilities program.

This past year, in-situ dual ion irradiation in the TEM of lift-out samples with temperature control of better than $\pm$1°C up through 500°C was demonstrated, and in-situ dual ion beam irradiation is now in operation.

Respectfully submitted,

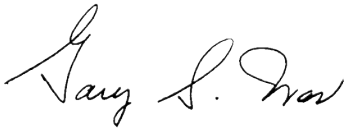

Gary S. Was, Director

Research Projects

Nuclear Science User Facility (NSUF) Projects

VARIABILITY IN HEAT-TO-HEAT RADIATION TOLERANCE OF ADDITIVELY MANUFACTURED HT-9 FERRITIC/MARTENSITIC STEELS

P. Xiu[1], N. Sridharan[2], K.G. Field[1]
[1]Department of Nuclear Engineering and Radiological Sciences, University of Michigan
[2]Lincoln Electric-India, India

Ferritic martensitic (FM) steels are candidate materials for high-dose applications in advanced nuclear reactor power applications due to their low swelling rates. FM steels are known to have gross changes in materials performance in these high dose applications due to irradiation hardening, helium embrittlement, and swelling. The use of additive manufacturing, which includes powder-blown laser directed energy deposition (DED), is gaining increasing acceptance for consideration in the production of commercial nuclear reactor components. To date, little details regarding the performance of additive manufactured HT-9 in reactor environments and even less on the heat-to-heat or batch-to-batch variability exist in the literature. Here, a follow on to previous irradiations was completed to investigate heat-to-heat and heat treatment effects on radiation responses of DED produced HT-9.

A FM steel, HT-9, was produced using powder-blown laser DED at Oak Ridge National Laboratory's Manufacturing Demonstration Facility (MDF) and then processed using two heat treatments that mimic those used in traditional processing routes. After that, the as-built, ACO3 and FCRD materials were irradiated at the Michigan Ion Beam Laboratory (MIBL) to a total damage dose of 50 displacements per atom (dpa) at 460°C using Fe^{2+} ions to rapidly assess the radiation tolerance of HT-9 DED material.

Figure 1 below shows the preliminary results of the irradiated HT-9 DED material using Scanning Transmission Electron Microscopy (STEM) to image the dislocation loops after irradiation. A high density of dislocation loops exists in the (a) as-built and (c) FCRD samples whereas only dislocation loops of <100> type and dislocation networks exist in the (b) ACO3 sample after the irradiation. Precipitates exist in all the irradiated samples, and their type will be determined at later date using Energy Dispersive X-ray Spectroscopy (EDS) and Atom Probe Tomography (APT). The preliminary results shown here currently show consistent results with previous results reported on a previous heat of DED produced HT-9 irradiated to the same conditions at MIBL in calendar year 2019.

This work was supported by the U.S. Department of Energy, Office of Nuclear Energy under DOE Idaho Operations Office Contract DE-AC07- 051D14517 as part.

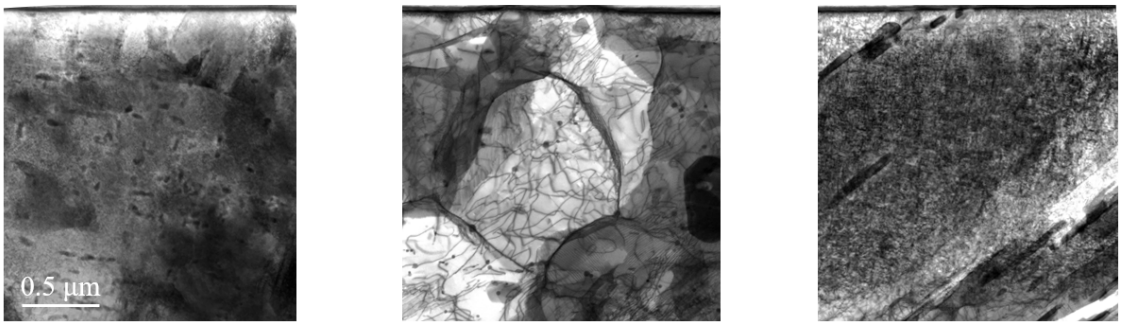

(a) (b) (c)

STEM-BF images showing the microstructures of additive manufactured (a) as-built (b) ACO3 heat-treated and (c) FCRD heat-treated HT-9 alloys after 5 MeV Fe^{2+} ion irradiation to 50 dpa at 460°C. All scale bars identical.

SILVER DIFFUSION IN TRISO REPRESENTATIVE FB-CVD SIC

T.J. Gerczak[1], R.L. Seibert[1], N. Sievers[2], O. Toader[3]
[1]Nuclear Fuel Materials Group, Oak Ridge National Laboratory
[2] Institute of Critical Technology and Applied Science, Virginia Tech University
[3]Department of Nuclear Engineering and Radiological Sciences, University of Michigan

Understanding fission product diffusion in representative materials of the tristructural isotropic (TRISO) fuel system is critical to predicting performance. The effort described herein is a subset of a larger project exploring diffusion in the pyrocarbon (PyC)/silicon carbide (SiC) system [1]. Silicon carbide (SiC) substrates were ion implanted at the Michigan Ion Beam Laboratory's 400 kV inline implanter through the Department of Energy Nuclear Science User Facility (NSUF) access. Two substrates were implanted; polycrystalline SiC substrates and single crystal 4H-SiC substrates. The substrates were implanted with Ag^{+} at 400 kV and 300 °C to a fluence of $1 \cdot 10^{15}$ ions/cm^2 resulting in a peak implantation depth of ~100 nm. A fluidized bed chemical vapor deposited (FB-CVD) SiC layer was deposited on the implanted SiC substrates. The resulting system is a consistent silver diffusion source adjacent to a representative TRISO-SiC layer. The buried nature of the implanted silver source allows for high temperature thermal exposures where prior ion implantation studies have shown surface decomposition [2]. These implanted substrates have been subjected to thermal exposures at temperatures representative of TRISO-fuel safety and margin testing conditions (up to 1800 °C) and irradiation in the High Flux Isotope Reactor to understand radiation enhanced diffusion at temperatures relevant to TRISO operation [1]. Depth profiling is ongoing to capture the nature of the silver diffusion over a range in condition tested. Secondary Ion Mass Spectroscopy (SIMS) has been identified as the optimal method due to its exceptional sensitivity (parts-per-billion) and dynamic range. Evidence of thermal diffusion of silver in the representative FB-CVD SiC layer at 1700 °C, 150 h has been confirmed. Continued analysis will illuminate diffusion kinetics in the Ag/FB-CVD SiC system and the impact of irradiation on diffusion.

This research is being performed using funding received from the DOE Office of Nuclear Energy's Nuclear Energy University Program through a joint NEET/NEUP R&D with NSUF access award (Project 16-10764).

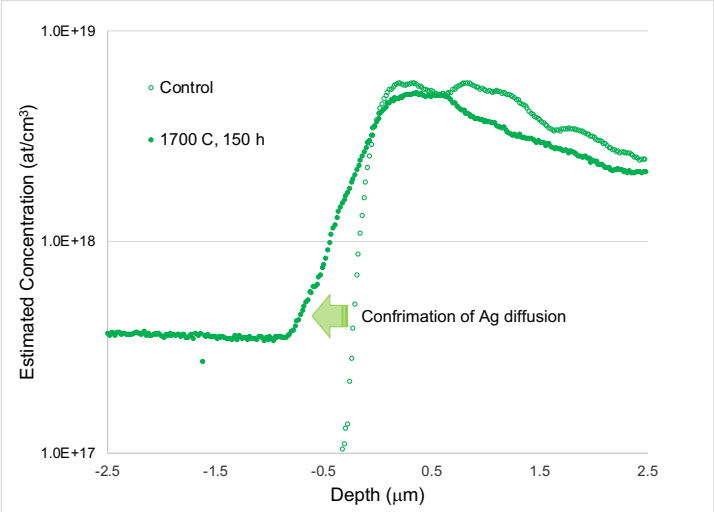

SIMS depth profile identifying diffusion into the representative FB-CVD SiC coating layer, 1,700°C for 150 h.

1. Gerczak, T.J., Campbell, A.A., Hu, X., Hunn, J.D., Jolly, B.C., Seibert, R.L., and Schumacher, A.T., *Preparation of Diffusion Couples for Irradiation and High-Temperature testing of Representative TRISO PyC/SiC*. ORNL/TM-2018/1012, 2018. Oak Ridge: Oak Ridge National Laboratory.
2. Friedland, E., Malherbe, J.B., van der Berg, N.G., Hlatshwayo, T., Botha, A.J., Wendler, E., and Wesch, W., "Study of silver diffusion in silicon carbide," *Journal of Nuclear Materials* 2009. 389(2): pp. 326–331

SCC IN Fe- AND Ni-BASED WELDMENTS FOR LWR SUSTAINABILITY

B.J. Heuser,[1] X. Bai,[2] B. Spencer,[3] and G.S. Was[4]
[1]Department of Nuclear, Plasma, and Radiological Engineering, University of Illinois
[2]Department of Materials Science and Engineering, Virginia Tech
[3]Fuels Modeling & Simulation, Idaho National Laboratory
[4]Department of Nuclear Engineering and Radiological Sciences, University of Michigan

The objective of this project is to provide experimental data on the performance of Alloy 308/309 and 82/182 weldments during exposure to environmental factors typical of normal LWR operation in support of the LWRS Program. In particular, the work scope is designed to determine inter-granular stress corrosion cracking (IGSCC) susceptibility with respect to radiation damage and LWR primary coolant chemistry. The goal is to correlate crack initiation and IGSCC to 1) grain boundary orientation, 2) local grain boundary chemistry and oxidation, 3) and localized deformation, and 4) dpa displacement cascade damage. The experimental protocols are designed to separate the effect of irradiation and associated radiation damage from environmental factors such as LWR water chemistry and applied load and to determine the synergistic effect of irradiation, water chemistry, and tensile stress. In addition, modeling activities are proposed that capture salient features of the materials response of these alloys to LWR environments. The combined experimental and computational methodology is anticipated to improve the predictive capability of Grizzly using a novel extended finite element method (XFEM). The proposed project will be supportive to the LWRS Program in two ways. First, it will expand the knowledge base to include the behavior of weldments found in LWRs. Second, it will serve as input into a modeling component to this project, which in turn will lead to enhanced predictive capability of Grizzly.

We have initiated SSR immersion testing of an EPRI 508LAS-304L weldment under different LWR water chemistry conditions using the UIUC recirculating loop autoclave. In addition, the second set of proton irradiation experiments were performed at the MIBL in July 2019. The figures below show four tensile specimens and six TEM specimens mounted prior to the irradiation experiment (left) and a thermal image 360 C. These specimens were successfully irradiation at 360 C to approximately 5 dpa (quick K-P model calculation via TRIM calculated at 60% depth of the Bragg peak). These specimens have undergone subsequent SSR immersion testing. Additional proton irradiations are planned.

This work was supported by the U.S. Department of Energy, Nuclear Energy University Programs under contract DE-NE0008699.

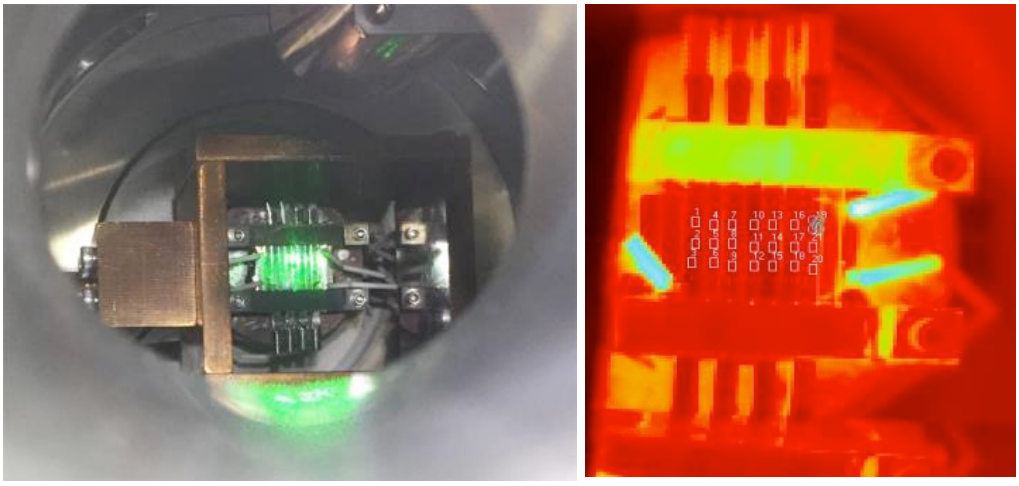

Mounted tensile and TEM specimens prior to proton irradiation at 360 C to approximately 5 dpa.

FISSION PRODUCT TRANSPORT IN SIC UNDER IRRADIATION

Z. Jiao, N. Chen, F. Gao, G.S. Was
Department of Nuclear Engineering and Radiological Sciences, University of Michigan

The objective of this research is to measure diffusion coefficients of fission products (FPs) in SiC under irradiation conditions, as well as synergistic effects of radiation damage, and fission product behavior at the IPyC/SiC interface. Molecular dynamics simulations are used to validate experimental data and determine the atomistic diffusion mechanisms to further improve empirical models used in the PARFUME code to predict FP release in TRISO fuel.

Silver was implanted into SiC at low (RT) and high (1120°C) temperature to study the silver transport behavior during the implantation process. Silver implantation was conducted using the 1.7 MV accelerator at Michigan Ion Beam Laboratory (MIBL) with 2 MeV Ag++. A high temperature irradiation stage that is capable of 1200°C was used. The peak accumulated dose was ~50 dpa due to silver self-irradiation. Distribution of Ag in SiC was characterized using Rutherford Backscattering Spectrometry (RBS) at MIBL and the secondary ion mass spectrometry (SIMS) at Surface Science Western, University of Western Ontario. Figure below shows the distribution of Ag in SiC implanted at RT and 1100°C as compared to the SRIM prediction. The loss of Ag at 1120°C indicates that mobility of Ag may be high during high temperature implantation. The role of Ag self-irradiation in promoting Ag mobility at high temperature is demonstrated in this experiment.

Support of this work was provided by DOE NEUP under award # DE-NE0008519.

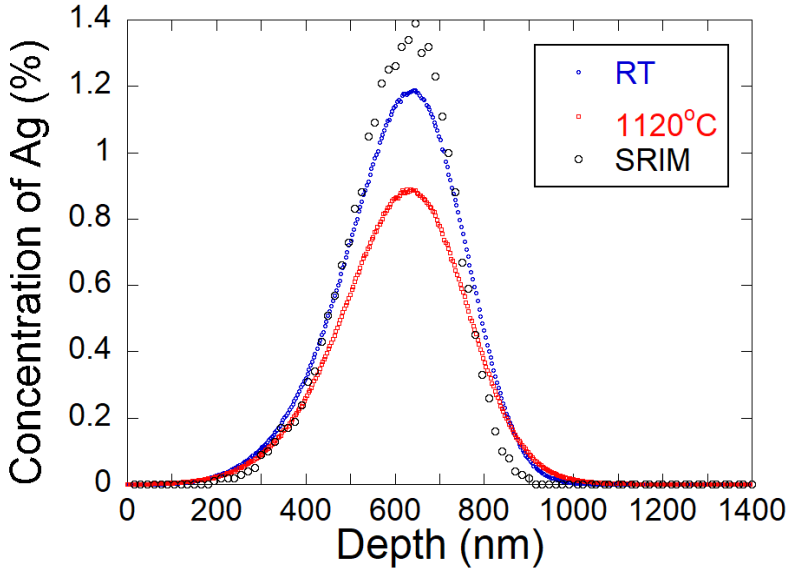

Distribution of Ag in SiC implanted at RT and 1120°C as compared to the SRIM prediction.

IN-SITU RESISTANCE MEASUREMENTS OF AEROSOL JET PRINTED SILVER UNDER He^{++} IRRADIATION

K. Fujimoto[1,2], T. Unruh[2], D. Estrada[1], M. McMurtrey[2], O. Toader[3] and G.S. Was[3]
[1]Micron School of Materials Science and Engineering, Boise State University
[2]Idaho National Laboratory
[3]Department of Nuclear Engineering and Radiological Sciences, University of Michigan

This study served as an extension to a previously completed Rapid Turnaround Experiment (RTE) where the effects of He^{++} on the electrical resistance of aerosol jet printed (AJP) silver was investigated. The motivation for these studies is to facilitate a graded approach of rapidly down selecting the library of materials compatible with additive manufacturing techniques for the development of advanced in-pile sensors. For reference, preliminary results for the electrical response of printed silver to He^{++} irradiation was a decrease in resistance at 0.01, 0.05 and 0.25 displacements per atom (DPA). For the initial study, resistance measurements were performed ex-situ.

Modifications to the first experiment included a target of 1.0 DPA, the use of alumina and sapphire substrates to investigate substrate effects, and an experiment set-up that allowed for in-situ resistance measurements to monitor the effects of He^{++} irradiation in real-time. Similarities to the initial experiment include the use of a four-point structure for electrical characterization, and printing was performed with an Aerosol Jet 200 system. Alumina and sapphire samples were prepared at Boise State University, and began with a pre-processing of both substrates to include O_2 plasma etch at 100 W for 60 sec. Post-processing involved sintering of printed structures at 350 °C for 60 minutes, and the attachment of 0.1 mm Kapton insulated copper wire with Epotek H20E cured at 120 °C for 15 minutes.

To investigate the irradiation response of He^{++} two total irradiation experiments were performed using the 1.7 MV Maize Tandem particle accelerator to achieve a minimum of 1.0 DPA on AJP silver printed on an alumina and sapphire substrate. In-situ resistance monitoring was made possible with the use of custom cables fabricated by MIBL, and by utilizing National Instruments USB-4065 Digital Multimeters. The beam energy was selected to ensure that He^{++} irons fully penetrated the printed structures, and temperature control was made with thermocouples to ensure that the irradiation did not exceed 350 °C. An example of the sample set-up can be found in Figs. a-b. To ensure that only the irradiation effects on printed materials was investigated, an area between the pads was selected for irradiation, which is made visible with the gray area in Fig.c. The discoloration of the alumina substrate is a result of the irradiation process.

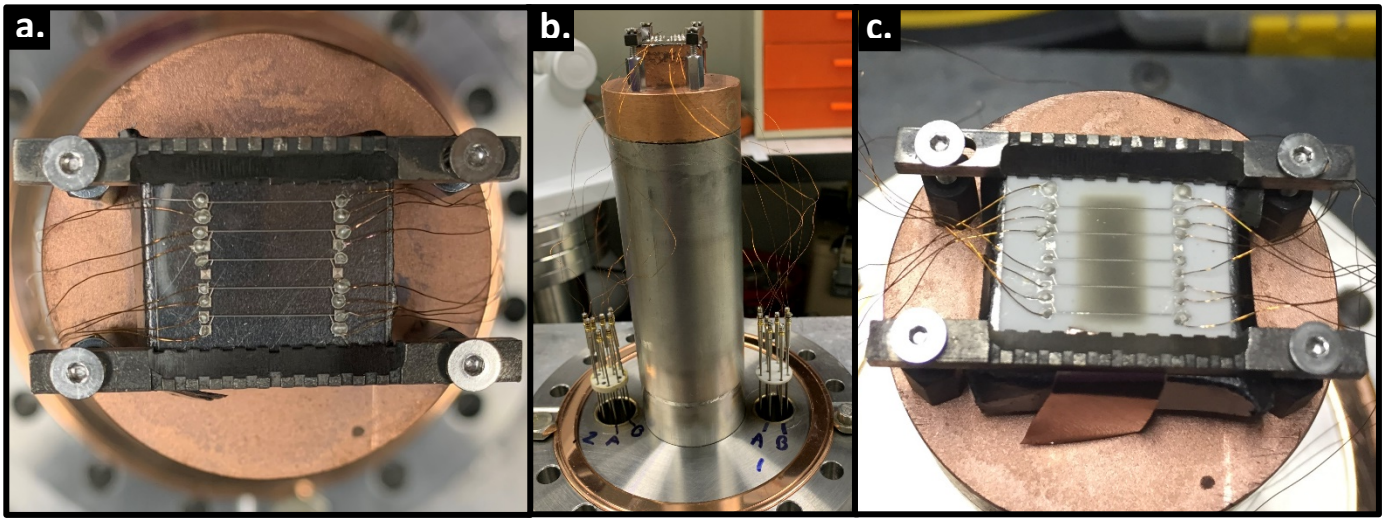

Sample irradiation stage demonstrating (A) AJP four-point silver structures on sapphire with attached copper wire leads, (B) attachment strategy for in-situ monitoring of electrical resistance with copper wire leads attached to 10-pin feedthroughs, and (C) post-irradiation AJP four-point silver structures where the discolored region makes visible the irradiated area of the AJP four-point structures.

RADIATION TOLERANCE OF ODS AND FeCrAl ALLOYS JOINED BY CAPACITOR DISCHARGE RESISTANCE WELDING

C.R. Lear[1], B.P. Eftink[1], T.J. Lienert[2], S.A. Maloy[1]
[1] MST-8: Materials Science in Radiation & Dynamics Extremes, Los Alamos National Laboratory
[2] T.J. Lienert Consulting, LLC, Los Alamos, NM
UNCLASSIFIED, LA-UR-20-XXXXX

Nano-structured, oxide dispersion strengthened (ODS) ferritic alloys have shown improved resistance to high temperature oxidation, creep, and radiation damage than conventional cladding materials for light water reactors (e.g., Zircaloy). However, joining these materials for structural use has been troublesome. Substantial heat input and local melting during common fusion welding degrade material performance (1) by coarsening grains and (2) by promoting agglomeration, non-uniform redistribution, or simple growth of oxide particles in the melt region. Solid-state welding (SSW) techniques, with lower peak temperatures and lack of melting, are thus a high priority. Capacitor-discharge resistance welding (CDRW) is particularly promising for SSW of cladding, as it can more easily accept small and varied sample geometries than friction stir welding and offers exceptionally brief (and thus less deleterious) thermal cycles than pressure resistance welding. In this study, FeCrAl-ODS joints prepared using CDRW were irradiated with protons or self-ions to investigate the effects of weld-induced microstructural evolution on radiation resistance. CDRW experiments were carried out at the Edison Welding Institute in Columbus, OH using ~1 cm diameter, ~0.5 mm wall thickness B126Y (FeCrAl) tubes and MA956 (ODS) caps, as shown in Fig. a. Weld conditions were varied in terms of load, discharge current, and discharge pulse time. CDRW joints were inspected by eye for melting or partial fusion and further characterized using light optical microscopy, scanning electron microscopy, and electron backscatter diffraction (EBSD). EBSD orientation maps, as shown in Fig. b, revealed exceptionally narrow layers of mechanically affected and recrystallized material along the weld line (~100 and 25 μm thick, respectively).

Additional welds were prepared using the two most promising parameter sets and sectioned parallel to the tube diameter, producing many flag-like samples for irradiation. Samples for each irradiation condition were ground to a uniform thickness using SiC papers, polished with 0.04 μm colloidal silica suspension, and electropolished at -35 ºC in a 5 vol% perchloric acid in methanol solution. Irradiations were performed at the University of Michigan's Michigan Ion Beam Laboratory (1.2 MeV H^+, 360 ºC, 1 and 5 dpa) and at the University of Wisconsin's Ion Beam Laboratory (3.7 MeV Fe^{2+}, 350 and 450 ºC, 10 and 100 dpa), with the former focused on chemical and phase stability effects and the latter on swelling. Microstructural evolution with irradiation was characterized using transmission electron microscopy. While defect characterization is still on going, nanoparticles in the MA956 material were not significantly coarsened by proton irradiation up to 5 dpa – even in weld affected material, see Fig. c. This supports the above finding that CDRW joining allows for complete sealing between parts with minimal microstructural impact.

This work was supported by the U.S. Department of Energy, Office of Nuclear Energy under DOE Idaho Operations Office Contract DE-AC07- 051D14517 as part of a Nuclear Science User Facilities experiment.

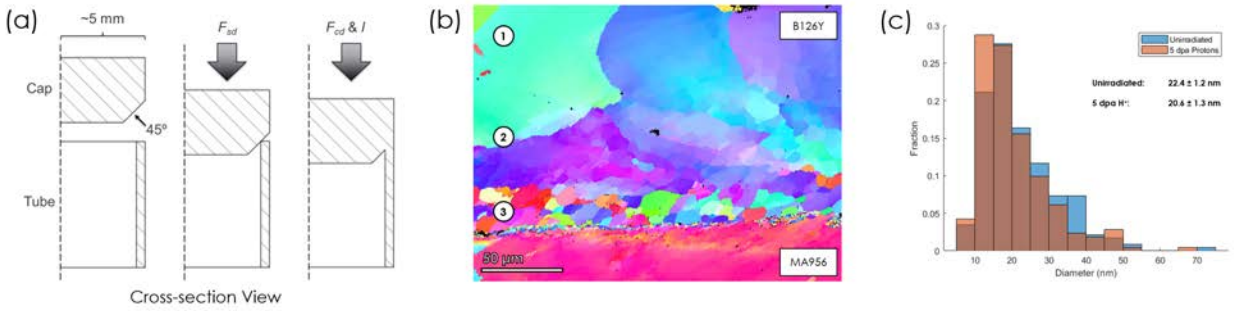

(a) Cross-sectional schematic of the CDRW process. (b) EBSD orientation map of grain structure across the weld line, highlighting (1) base, (2) mechanically affected, and (3) recrystallized materials. (c) Histograms of nanoparticle diameters in as-welded and 5 dpa H^+ irradiated MA956, suggesting some but insignificant refinement.

IRRADIATION EFFECTS ON SENSOR MATERIAL COMPOSITION USING ION IRRADIATIONS AND HIGH-THROUGHPUT COMBINATORIAL MATERIAL TESTING

N. Kempf[1], Y. Zhang[1], M. McMurtrey[2]
[1]Department of Aerospace and Mechanical Engineering, University of Notre Dame
[2]Idaho National Laboratory, United States

The goal of this work is to develop rapid, high-throughput screening and discovery of materials for improved in-pile instrumentation. Combinatorial materials science combined with high-throughput screening methodology offers potential for developing radiation-resistant sensor materials for nuclear energy applications through the synthesis and screening of large numbers of compositions and processing conditions in a single process. The combinatorial materials synthesis coupled with an automated screening process enables us to identify the optimal materials composition and processing conditions that yield both desired properties and required irradiation resistance in the most efficient and economic manner. This preliminary work studies the ion irradiation effect on the thermal and thermoelectric properties of a Zinc Tin Nitride (ZTN) combinatorial film of gradient composition. The combinatorial ZTN film was irradiated to 0.035 dpa with 4.5 MeV alpha particles that yielded a uniform damage region through the thickness of the ~1 μm-thick film. For the first time, microscale thermal conductivity and Seebeck coefficient were mapped before and after ion irradiation of a combinatorial film with a custom thermal scanning microprobe.

A long copper strip was suspended along the length of the film in preparation for irradiation. After irradiation, the copper strip was removed to expose a length of the non-irradiated film adjacent to the irradiated region. This allowed measurement of the irradiated and non-irradiated sections of the film at the same time, eliminating errors introduced by measurement at different times, such as oxidation and contamination. The results of scanning thermal microscopy show a significant increase in Seebeck coefficient along the length of the film with a maximum increase of 50% near Zn/(Zn + Sn) = 0.72. A relatively moderate decrease in thermal conductivity was found with uniform suppression from the Zinc-poor edge to around Zn/(Zn + Sn) = 0.695, beyond which point decreases in conductivity gradually subside. The relatively uniform increase in Seebeck coefficient is likely due to compositional changes. It is hypothesized that preferential sputtering of tin and/or nitrogen occurred during ion irradiation, effectively lowering the carrier concentration and increasing Seebeck coefficient. The decrease in thermal conductivity is attributed to a combination of this composition change along with the introduction of irradiation-induced defects that act as phonon scattering sources, reducing phonon mobility and decreasing conductivity.

This work was supported by the U.S. Department of Energy, Office of Nuclear Energy under In-Pile Instrumentation in the Nuclear Energy Enabling Technology: Advanced Sensors and Instrumentation program.

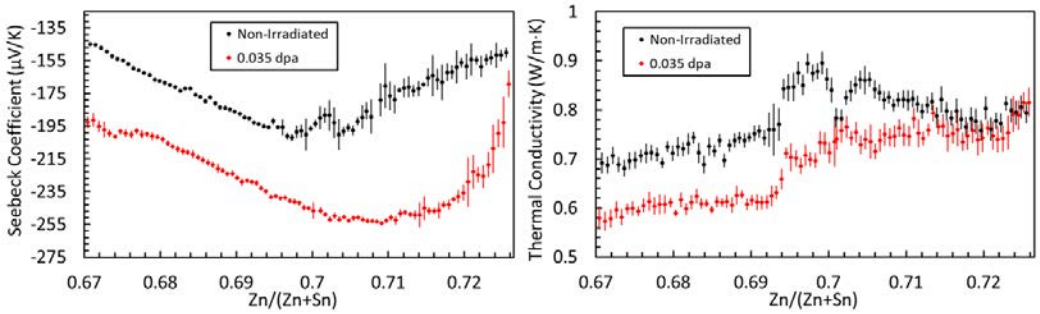

Scanning thermal microscopy results showing Seebeck coefficient (left) and thermal conductivity (right) of the irradiated and non-irradiated combinatorial ZTN film. Scale bars are 95% confidence intervals.

TEMPERATURE SHIFT EVALUATION FOR G-PHASE NANOCLUSTER EVOLUTION IN FERRITIC/MARTENSITIC ALLOYS

M.J. Swenson, S.B. Adisa
Department of Mechanical Engineering, University of Idaho

The objective of this project is to validate the temperature shift requirements for irradiation-induced nanocluster evolution in three separate ferritic-martensitic alloys, as predicted by two unique nanocluster evolution calculation models**.** Recent analysis of F/M alloy T91 at the same irradiation conditions demonstrate varying results in nanocluster evolution (Fig. 1) with the higher dose rate irradiation resulting is coarser nanocluster distribution. This result suggests the need for an experimental temperature shift when irradiating with charged particles at higher dose rates to accurately emulate neutron irradiation.

Two different calculation models are adapted to simulate irradiation-induced nanocluster evolution in F/M alloys T91, HCM12A, and HT9. First, cluster dynamics is used through only modifying the parameters to reflect our irradiation conditions (Fe^{2+} or neutron irradiation at 500 °C) and the alloy compositions. The cluster dynamics model reasonably simulates the nanocluster evolution up to 3 dpa (Fig. 2a and 2b), predicting larger nanoclusters with self-ion irradiation. Through evaluation of temperature sensitivity, the model also predicts that Fe^{2+} irradiation at a revised temperature of 360–380 °C would result in close emulation of the neutron irradiation result at 500 °C, suggesting a negative temperature shift is merited for Fe^{2+} irradiation. This negative temperature shift is corroborated with another model based on rate theory and the work of Nelson, Hudson, and Mazey (NHM) describing nanocluster radius (r) evolution over time (t). Both models are in good agreement with the experimental result and predict a negative temperature shift for higher dose rate irradiation. To validate the temperature shift prediction of the two models, we conducted self-ion irradiation with 5 MeV Fe^{2+} ions to 3 dpa at 370°C on the aforementioned alloys at the Michigan Ion Beam Laboratory (MIBL). APT characterization following Fe^{2+} ion irradiation at 370 °C at 3 dpa shows the size and number density of solute nanoclusters is similar to that obtained following neutron irradiation at 500 °C at the same dose. This result validates the efficacy of the two models and suggests a negative temperature shift is required for Si-Mn-Ni-rich solute clusters in F/M alloys exposed to low dose.

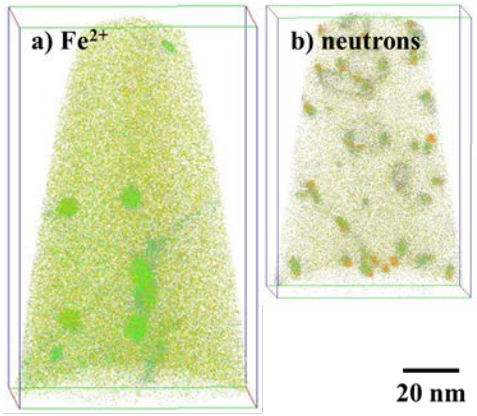

Figure 1. Atom probe maps of T91 showing Si, Mn, Ni, and Cu clustering following irradiation to 3 dpa at 500°C with a) 5 MeV Fe^{2+} ions, or b) fast neutrons.

This work was supported by the U.S. Department of Energy, Office of Nuclear Energy under DOE Idaho Operations Office Contract DE-AC07- 051D14517 as part of a Nuclear Science User Facilities experiment 18-1210.

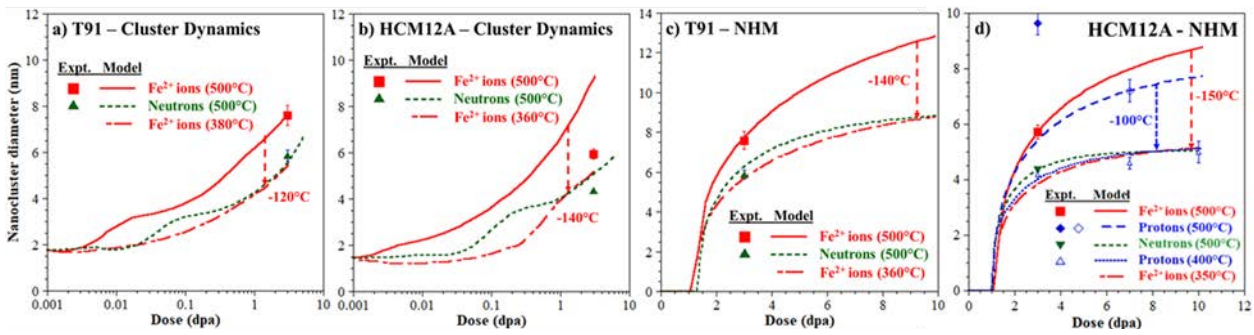

Figure 2. Experimental results compared with model simulations of Si-Mn-Ni-rich nanocluster evolution in alloys T91 and HCM12A using a-b) cluster dynamics, and c-d) NHM rate theory models.

Non-NSUF Projects

HIGH FIDELITY ION BEAM SIMULATION OF HIGH DOSE NEUTRON IRRADIATION

S. Taller, Z. Jiao, K. G. Field, G.S. Was
Department of Nuclear Engineering and Radiological Sciences, University of Michigan

Traditional research efforts to understand radiation-induced processes in materials requires years of comprehensive post-irradiation characterization effort of test reactor produced neutron irradiated material. The same levels of radiation damage can be achieved using heavy ion irradiation under tightly controlled conditions in days or weeks instead of years in a nuclear reactor, albeit with several challenges. The purpose of this work is to address these challenges in using ion irradiation experiments as a surrogacy for neutron irradiation.

Several dual ion irradiations were performed using 5.0 MeV defocused Fe^{++} ions to damage the material and simultaneously injecting He^{++} ions in a fixed ratio to emulate gas buildup from nuclear transmutation reactions. Bars of T91 were dual ion irradiated up to 35 dpa with 0.22 appm helium per dpa from 420°C to 570°C to compare with multiple conditions from the BOR-60 fast reactor to the same level of damage and examine the role of temperature on the irradiated microstructure. These specimens are being examined with transmission electron microscopy and atom probe tomography to determine the effects of simultaneous helium injection and radiation damage on the irradiated microstructure of these materials.

EDS-based line scans were collected using the JEOL 2100F at the Michigan Center for Materials Characterization across the lath boundary with a spacing of 1 nm between points and a count rate of approximately 1300-1400 counts per second and a dead time of 1-2%. Each line scan was collected until the count under the Fe-K_α peak was greater than 10,000, corresponding to a 1% error in the Fe concentration. The enrichment of Ni at grain boundaries was found to be quantitatively similar between dual ion irradiated T91 and BOR-60 irradiated T91 with a temperature shift of +60°C. The lack of significant enrichment in Cr or Si is qualitatively consistent with invariance theory.

This work is supported by the U.S. Department of Energy under award DE-NE0000639. This research was performed, in part, using instrumentation provided by the Department of Energy, Office of Nuclear Energy, Nuclear Technology R&D (formerly Fuel Cycle R&D) Program, and the Nuclear Science User Facilities.

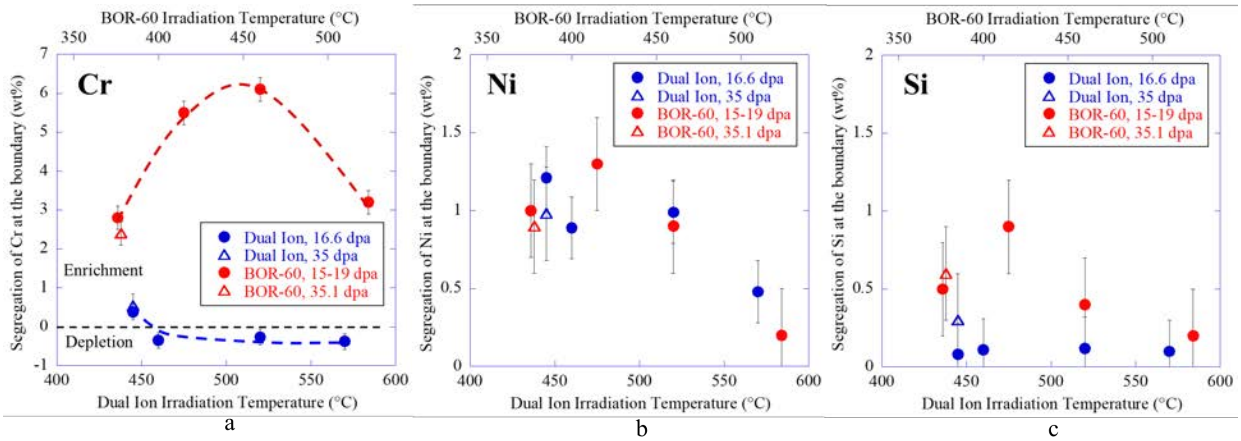

Irradiation dose and temperature effect on the segregation of (a) Cr, (b) Ni, and (c) Si at the grain boundary for dual ion irradiation T91 and BOR-60 irradiated T91. *Taller et al. JNM 527 (2019)*

EFFECTS ON IRRADIATION ON OXIDE GROWTH AND DISSOLUTION OF 316L STAINLESS STEEL

R.D. Hanbury, G.S. Was
Department of Nuclear Engineering and Radiological Sciences, University of Michigan

Two in situ proton irradiation corrosion experiments on 316L heat 626032 were completed in the past year. Irradiations were completed using Wolverine, the 3 MV tandem accelerator, on beamline 3. Both irradiation experiments used a 5.4 MeV raster scanned H^+ beam, $7x10^{-7}$ dpa/s at the corrosion surface, ~700 kGy/s radiolysis in 320˚C, 13.1 MPa, 3 wppm H_2 pure water and a 24 h or 72 h exposure time. Irradiation samples were prepared with 17-4PH backing material to reduce sample deformation and radioisotope content and a 316L heat 626032 bar mounted on the sample side to create a radiolysis analysis surface. Both the sample disc and bar were hot-implanted with 400 keV helium at 550˚C to 10^{16} He/cm^2 prior to exposure, producing a bubble marker layer for measuring oxide dissolution.

Following a 24 hr exposure in 320°C high purity water containing 3 wppm H_2, oxide thickness and composition were noted to be very similar in the presence of active radiolysis with or without displacement damage. Without radiation effects, the inner oxide thickness was much greater and more uniform in composition. The 72 h experiment results are still pending characterization.

This work is supported by EDF Contract No. 8610-5920005571, the University of Michigan College of Engineering, and NSF grant #DMR-0723032 for the JEOL 2100F.

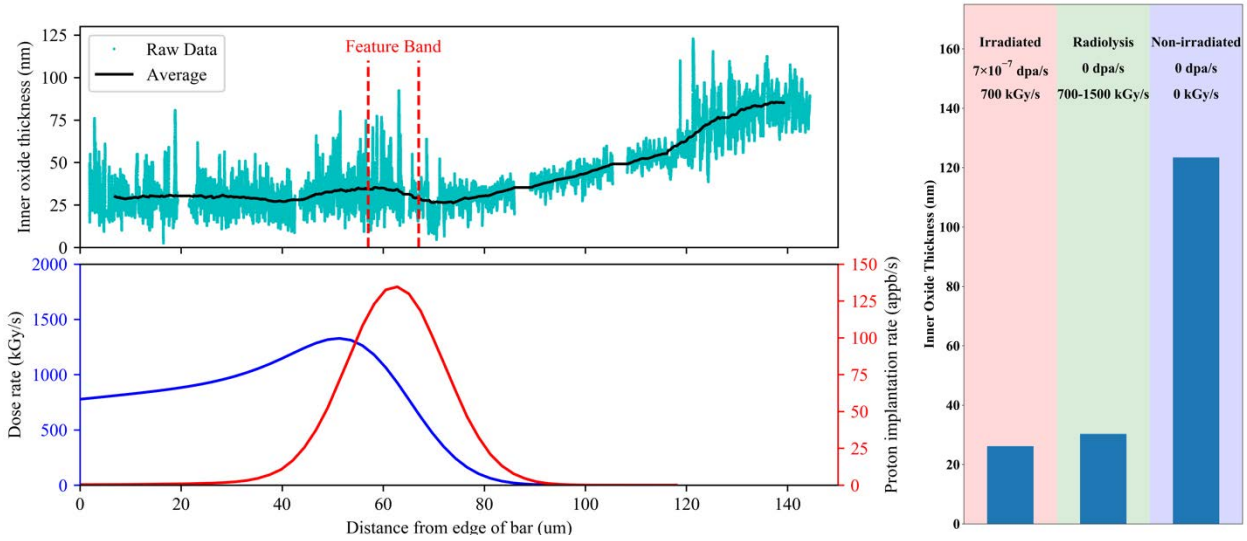

Measurements of inner oxide thickness across the radiolysis isolation region as a function of dose rate (a) and averaged for each separate region (b).

USING ION IRRADIATION TO EXTEND THE DAMAGE LEVEL OF NEUTRON IRRADIATED STAINLESS STEELS

S. Levine[1], Z. Jiao[1], C. Parish[2], G.S. Was[1]
[1]Department of Nuclear Engineering and Radiological Sciences, University of Michigan
[2]Oak Ridge National Laboratory

Ion irradiated microstructures are extremely sensitive to initial composition and heat treatment. Unfortunately, unirradiated material of the same heat already being used in reactor is rarely available. Thus, the objective of this study is to determine the efficacy of irradiating neutron irradiated material (preconditioned samples) with heavy ions to simulate high damage levels.

The samples for these experiments were 304L stainless steel fabricated for a BWR core shroud. These samples were initially irradiated in the BOR-60 fast reactor at 320°C at a dose rate of 9.4 x 10^{-7} dpa/s (E > 0.1 MeV) to doses of 5.5, 10.2, and 47.5 dpa. In the Michigan Ion Beam Laboratory, irradiation damage was added to 5.5 dpa samples using a defocused beam of 9 MeV Ni^{3+} ions at a dose rate of ~10^{-3} dpa/s at 380, 400, and 420°C so that a final dose of 47.5 dpa was reached. A comparison of dislocation loops, precipitates, and radiation induced segregation (RIS) between the 47.5 dpa BOR-60 samples and the ion+neutron irradiated samples was subsequently conducted. Experiments performed at 400°C resulted in loop densities and sizes as well as grain boundary compositions similar to the BOR-60 irradiated samples; however, Cu precipitates were unstable and the nucleation of G-phase was inhibited under the high damage rate of ion irradiation.

This material is based upon work supported under an Integrated University Program Graduate Fellowship. In addition, this work is supported by the U.S. Department of Energy Nuclear Energy University Program (NEUP) and Nuclear Science User Facilities (NSUF) under grant DE-NE0008520.

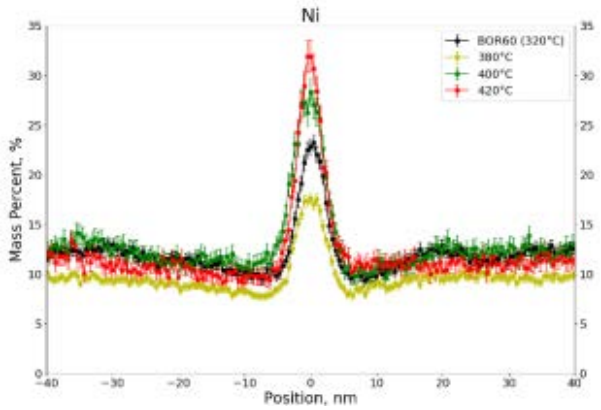

Figure 1. Segregation of Ni at high angle, random grain boundaries at 47.5 dpa measured using STEM-EDS with an FEI Talos F200X for the BOR-60, 380, 400, and 420 °C irradiation conditions.

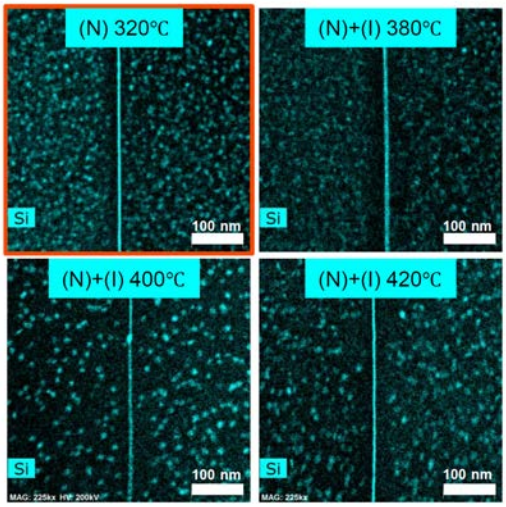

Figure 2. Si based solute clusters at 47.5 dpa observed using STEM-EDS with an FEI Talos 200X for the BOR-60, 380, 400, and 420 °C irradiation conditions where (N) indicates irradiation by neutrons and (N)+(I) indicates ion+neutron irradiation.

LOCALIZED DEFORMATION AND INTERGRANULAR FRACTURE OF IRRADIATED ALLOYS UNDER EXTREME ENVIRONMENTAL CONDITIONS

D.C. Johnson[1], G.S. Was[1], B. Kuhr[2], D. Farkas[2], R. Mo[3], I.M. Robertson[3]
[1]Department of Nuclear Engineering and Radiological Sciences, University of Michigan
[2]Department of Materials Science and Engineering, Virginia Tech University
[3]Department of Materials Science and Engineering, University of Wisconsin

The goal of this project is to determine the role of localized deformation in austenitic steel during irradiation assisted stress corrosion cracking (IASCC). The project is a collaboration between the University of Michigan, University of Wisconsin, and Virginia Tech University with the purpose of obtaining better understanding of the mechanisms involved in IASCC. Samples are being irradiated at the University of Michigan and strained in constant extension rate tensile (CERT) tests to study the cracking behavior. Atomistic models of the experiments are being developed by Dr. Farkas' group at Virginia Tech University, and irradiated samples will be strained in-situ in a TEM by Dr. Robertson's group at the University of Wisconsin.

This year, one irradiation was performed using 2 MeV protons at 360 °C on a 13Cr15Ni lab purity alloy in the Tandem Accelerator located in the Michigan Ion Beam Laboratory. The irradiation reached a damage level of 0.5 dpa to study the stress state developed in lower damage steels. Tensile bar samples from the irradiations were used to quantify the stress component normal to grain boundaries at discontinuous dislocation channel – grain boundary interaction sites, and then related to cracking. Samples were strained in high temperature argon (288°C) to produce many dislocation channels. These channels are either arrested at the grain boundary or transmit into the adjacent grain. In both cases, residual elastic stress values will be calculated using High Resolution Electron Backscatter Diffraction. Once stresses have been characterized, the stress values of this lower damage sample will be compared to the values observed in a sample made from the same heat of material, but irradiated up to 5 dpa to investigate if the higher damage results in a higher degree of strain localization and therefore higher levels of stress amplification as the dislocation channels interact with grain boundaries. Cracking was observed in the 5 dpa sample, however the 0.5 dpa sample should be below the generally observed threshold IASCC threshold of ~1 dpa for austenitic steels.

This research has been supported by the Basic Energy Science office of the U.S. Department of Energy under grant DE-FG02-08ER46525.

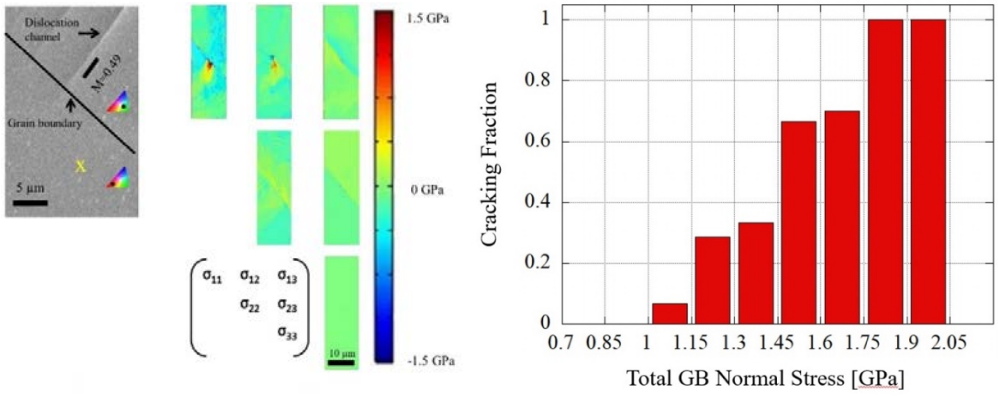

(a) Stress tensor calculated near a shown discontinuous channel-GB interaction site. Dependence of the cracking susceptibility on the magnitude of the stress acting normal to the grain boundary plane. (b) GB site cracking dependence on the total stress applied in a direction normal to the GB plane.

ION IRRADIATION OF Fe-15Cr MODEL ALLOY

K.N. Thomas, Z. Jiao, G.S. Was
Department of Nuclear Engineering and Radiological Sciences, University of Michigan

High-chromium ferritic-martensitic (F-M) alloys are a candidate material type for future nuclear power plants due to the corrosion resistance and low swelling under irradiation. However, with chromium concentrations above ~9% and at temperatures below ~500°C, the F-M alloys are susceptible to the formation of the Cr-rich α' precipitates. Research has shown that the α' precipitates can be formed under thermal aging, as well as neutron, electron, and proton irradiation, but there is difficulty in the α' precipitate formation under heavy ion irradiation due to ballistic dissolution.

Model alloy Fe-15Cr was irradiated at the Michigan Ion Beam Laboratory (MIBL) in a series of experiments. The 15Cr samples had been previously irradiated at MIBL last year with 2 MeV protons to 1 dpa at 400C at $1x10^{-5}$ dpa/s to establish an α' precipitate microstructure. The first experiment utilized 2 MeV protons to 2 dpa at 400°C at $1x10^{-5}$ dpa/s. This irradiation was to confirm the existing α' precipitate microstructure is at steady-state by 1 dpa. Further irradiations utilized 4.4 MeV $Fe^{2+/3+}$ at 400°C to 1 and 10 dpa over a range of damage rates ($1x10^{-5}$, $1x10^{-4}$, $3x10^{-4}$, and $1x10^{-3}$ dpa/s). The effects of the heavy ion irradiation on the α' precipitate was observed using APT to determine the effects of the damage rate. A damage rate limit was established for α' precipitates at 400°C in 15Cr between $1\text{-}3x10^{-4}$ dpa/s, above which α' precipitates are expected to completely dissolve or not nucleate.

This work is supported by the U.S. Department of Energy under award DE-NE0000639.

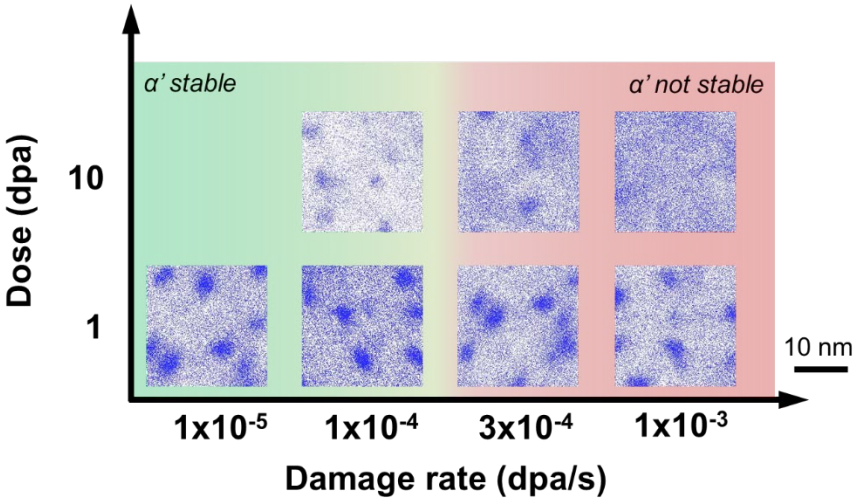

APT reconstruction of α' precipitates in Fe-15Cr for each heavy ion irradiation condition. At 1 dpa, α' is still present under all damage rates, but by 10 dpa, a clear damage rate limit is observed between $1\text{-}3x10^{-4}$ dpa/s, above which α' will completely dissolve or not nucleate.

ASSESSMENT OF SHADOW CORROSION MITIGATION COATINGS USING IN-SITU PROTON IRRADIATION-CORROSION TESTS

P. Wang[1], G. S. Was[1], K. Nowotka[2]
[1] Department of Nuclear Engineering and Radiological Sciences, University of Michigan
[2] Framatome GmbH

Shadow corrosion, as a type of irradiation-assisted galvanic corrosion between dissimilar metals, the shape of the component is often reproduced in the shape of an area of enhanced corrosion, suggestive of shadow casted by the component on the zirconium alloy surface. Shadow corrosion is also closely related to the channel bowing phenomena, which resulted in control blade interference due to channel distortion.

Several mechanisms have been proposed to explain the appearance of shadow corrosion, and the majority are related to the electrochemical nature of the Zircaloys. However, to date, shadow corrosion has only been observed on samples exposed in reactor. This implies the possible mechanisms by which radiation assists the shadow corrosion process; (1) by increasing the electrical and ionic conductivity of the oxide on Zr alloy, (2) by increasing the oxidizing species at the metal/oxide interface through creating radiolysis products. This project was aimed to use the existing spring-loaded wire design shown in Fig. 1, to assess the durability and effectiveness of the newly developed shadow corrosion mitigation coatings on Inconel 718.

In the figure, we have demonstrated that pre-oxidizing the metallic coating on Inconel 718 in an autoclave improves the resistance for shadow corrosion on a thicker coating, while the same pre-oxidizing process had minor effect on a thinner coating. The reference case represents the oxide thickness resulted from a proton irradiation without the Inconel 718 counter-electrode attached. This research was supported by the Framatome GmbH, Contract No.GF01/1019026112.

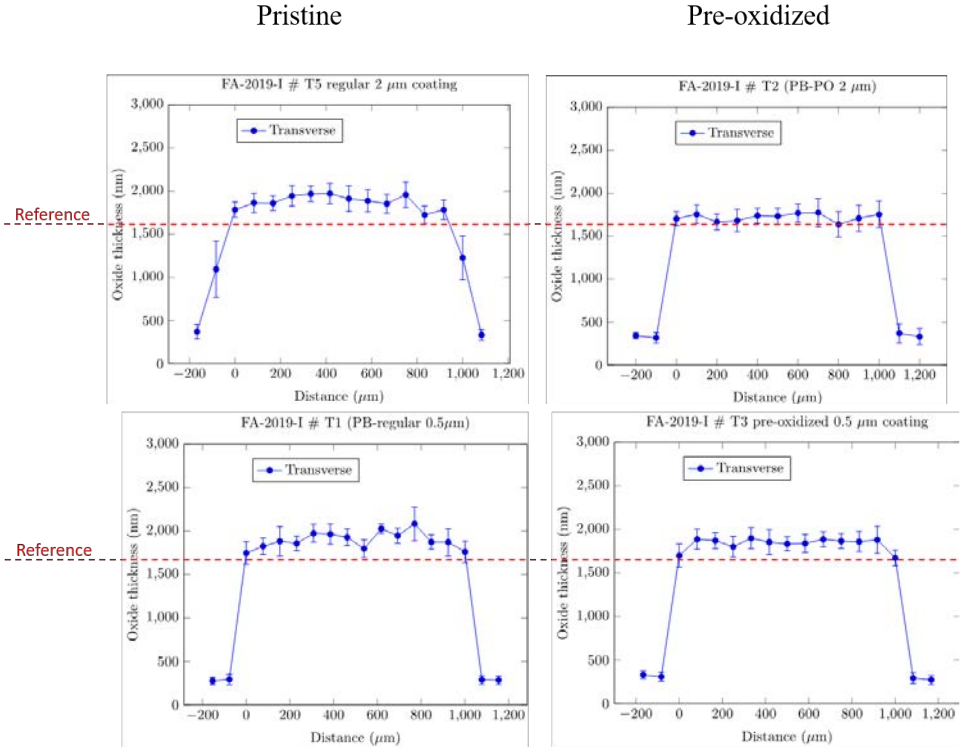

Oxide thickness profile across the in-situ irradiated-corrosion region, the resulting oxide thickness was compared between the pristine metallic coating and pre-oxidized coating at two oxide coating thicknesses.

THE INFLUENCE OF ION IRRADIATION ON THE CORROSION KINETICS OF ZIROCNIUM ALLOYS

P. Wang[1], G.S. Was[1], B. Kammenzind[2]
[1] Department of Nuclear Engineering & Radiological Sciences, University of Michigan
[2] Navel Nuclear Laboratory

The mechanistic understanding of zirconium alloy corrosion and hydrogen pickup in out of reactor testing has advanced the state-of-the-art of the field and provided insights in identifying promising alloys for use in reactors under extreme service duty conditions. However, despite similarities between autoclave and in-rector corrosion that allow the use of unirradiated material information and testing to identify potential alloys for service, processes that occur in the reactor are quantitatively and qualitatively different than those in an autoclave environment. The aim of this project is to combine both ion irradiation (both bulk and in-situ) and advanced characterization techniques to study the effect of irradiation on the corrosion kinetics of zirconium alloys. The research was focused on separate effects testing for the different mechanisms through which irradiation can affect corrosion, namely irradiation induced changes to the base material microstructure and microchemistry, changes to the water chemistry through radiolysis and irradiation effects on the oxide. A set of 2MeV proton irradiations was carried out on a Zircaloy-4 heat that NNL supplied and a Zr-1Nb alloy from another supplier. Samples with dimension of 2×20×1mm were irradiated to damage level of 0.5, 1.6 and 5 dpa at temperatures ranging from 280-350˚C. A heavy ion experiment was also performed on the same alloys to 1.6 dpa at 250 ˚C to promote amorphization of the SPP. The figure shows the TEM images and diffraction patterns between the completely amorphized SPP irradiated by Zr^{2+} ions and crystalline SPP that was unirradiated.

This work was supported by the Navel Nuclear Laboratory.

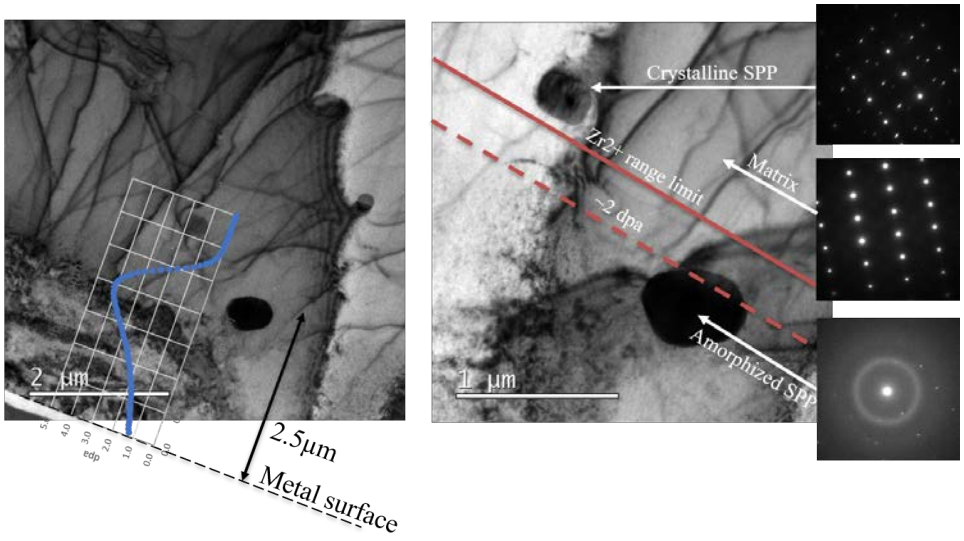

TEM and SAED images of Zr^{2+} ion irradiated Zircaloy-4 at 250°C, at a depth of 2.5μm below the metal surface (left), and within the range of the Zr^{2+} ion, the SPP was completely amorphized (right), indicated by the amorous ring pattern, whereas the SPP located outside of the ion range remained in its crystalline state indicated by its diffraction pattern which is a mixture of the diffraction spot of the SPP and the surrounding matrix.

MITIGATING IRRADIATION-ASSISTED STRESS CORROSION CRACKING BY RAPID ALLOY DEVELOPMENT VIA ADDITIVE MANUFACTURING

M. Song[1], X. Lou[2], L. He[3], Y. Zhang[4], and D. Schwen[5]
[1]Nuclear Engineering and Radiological Sciences, University of Michigan
[2]Department of Mechanical Engineering, Auburn University
[3]Characterization and Advanced PIE Division, Idaho National Laboratory
[4]Department of Engineering Physics, University of Wisconsin
[5]Fuel Modeling and Simulation, Idaho National Laboratory

Additive manufacturing (AM) techniques have been extensively explored for reactor applications to reduce supply chain, cost, and time to market. The AM techniques were originally considered for producing small parts such as fuel assemblies, control rod drive internals, advanced heat exchangers, and debris filter, but were quickly extended to larger parts for core internal and pressure vessels in small modular reactors (SMRs) or microreactors to shorten the fabrication time. Despite the promising future of AM techniques for nuclear applications, limited information is available on the properties, and thus, the reliability of the built parts under service conditions. During the past decades, electric power research institute (EPRI) has identified that void swelling, embrittlement, loss of fracture toughness, and irradiation-assisted stress corrosion cracking (IASCC) as the major degradation mechanisms in light water reactors for long term operation. Therefore, it is critical to evaluate the IASCC susceptibility of additively manufactured materials and develop new alloys to improve their resistance to IASCC.

Microalloyed 316L stainless steels (SSs) with the addition of Hf, Y, Ta, Zr elements were prepared by Auburn University. This group of materials served as control samples for the additively manufactured steel with the same composition. The materials were irradiated to 0.1, 0.3, and 1dpa using Wolverine accelerators with 2MeV protons at a temperature of 360℃. The experimental temperature was selected based on Mansur's invariance theory to compensate for the dose rate difference between neutron irradiation condition (~320℃ and 1×10^{-7} dpa/s) and proton irradiation. Irradiation hardening may serve as one of the simple indicators of radiation tolerance. All the irradiation induced loop, precipitates, and void can serve as barriers for mobile dislocation which further contribute to the irradiation hardening. Despite different responses of microalloyed 316L SS at lower damage levels, the irradiation hardening of different alloys tends to merge at 1dpa. Microstructural characterization is on-going to provide–further explanation. IASCC of these materials will be evaluated shortly.

This work is supported by the Department of Energy, Laboratory Directed Research & Development at Idaho National Laboratory under contract 19A39-071FP.

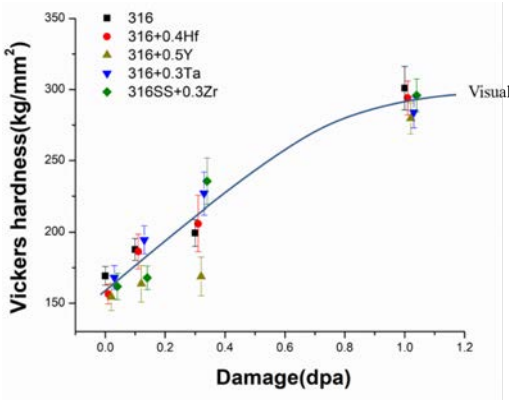

Dose-dependent irradiation hardening of microalloyed 316L SS with different oversized elements after 2 MeV proton irradiation to different damage levels at 360℃.

RAPID SIMULATION OF VOIDS SWELLING IN PWR INTERNALS

M. Song[1], K.G. Field[1], C. Topbasi[3], J.T. Busby[2], and G.S. Was[1]
[1]Nuclear Engineering and Radiological Sciences, University of Michigan
[2] Materials Science and Technology Division, Oak Ridge National Laboratory
[3] Electric Power Research Institute, Palo Alto, CA

In Dec. 4th, 2019, Nuclear Regulatory Commission (NRC) in the United States approved a subsequent license renewal for two units at Turkey Point Nuclear Reactors at Florida, marking an era of life extension of light water reactors beyond 80 years. The safe operation of a nuclear power plant during such an extension will strongly depend on the degradation of the material in the reactor core internals. The Electric Power Research Institute (EPRI) has identified the major degradation mechanisms in light water reactors for long term operation. These degradation mechanisms include void swelling, embrittlement, loss of fracture toughness, and irradiation-assisted stress corrosion cracking (IASCC). All of these degradation mechanisms are closely related to the microstructural evolution of structural materials under irradiation. Therefore, to predict and mitigate those degradations, the data and validated models for such high damage level is in desperate need. Ion irradiation is the only feasible approach identified to access such high damage regimes in short time. The goal of this project is to use self-ion (Ni^{3+}) irradiation to capture the growth processes at higher damage levels ~160 dpa of cold-worked 316L SS after the precursor nucleation processes are completed via PWR irradiations. Such a damage level corresponds to core internal material after 100 years of exposure.

Thin disks of 3 mm diameter and 0.2 mm thickness were cut from flux thimble tubes of a commercial nuclear power reactor with various neutron damage levels 0, 38-41, 72-75, and 100 dpa. Two irradiation experiments were performed on 38 dpa reactor irradiated samples using the Wolverine accelerator with 8 MeV Ni^{3+} ions at temperatures of 390 and 410°C to a damage level of 34 dpa. The total added dose in these two samples will be 72 dpa allowing a direct comparison with the reactor irradiated sample at a similar dose. The nanocavities, dislocation loops, and Ni-Si-rich clusters were very consistent between neutron and neutron + ion irradiated conditions. Radiation induced segregation results indicated that irradiation at 410°C seems a better condition because the major elements matches well with the trend of reactor radiation conditions, as provided in Figure a and b. RIS of Mo in both ion irradiation conditions failed to reproduce the trend of reactor radiation conditions. RIS of Si was required more investigation because that ion irradiation at 390°C matched well with 100 dpa reactor irradiated sample, while ion irradiation at 410°C agreed with 41 dpa reactor irradiated sample. However, none of them was consistent with the reactor irradiated 74 dpa samples. Further analysis is on-going.

This work was supported by the Electric Power Research Institute under contract number 10002154 and 10002164.

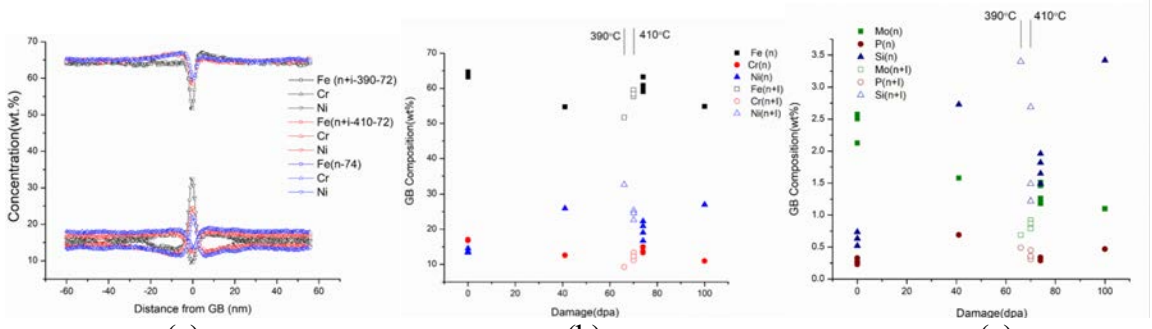

(a) (b) (c)

Radiation induced segregation in neutron and neutron+ion irradiated samples. (a) Grain boundary composition at a similar dose. Dose dependent GB composition of (b) Major elements and (c) Minor elements. Dpa levels were offset by 2 and 4dpa for ion irradiation conditions for the sake of clarity. In figure (a), the segregation data of 74 dpa reactor irradiation was plot with the profile with most segregation, which is more likely to be a random high angle grain boundary.

IRRADIATION EFFECTS IN FERRITIC-MARTENSITIC STEELS AT VERY HIGH DAMAGE LEVELS

D. Woodley, Z. Jiao, K. Sun, G.S. Was
Department of Nuclear Engineering and Radiological Sciences, University of Michigan

Understanding the microstructural evolution in ferritic-martensitic steels is important for predicting the safety and reliability of future reactors. Dual ion irradiation experiments have been performed on heat 84425 of HT9, a ferritic-martensitic steel, to examine the effects of increased damage level on bubbles and cavities. Irradiations were performed at the Michigan Ion Beam Laboratory with 5 MeV Fe^{++} ions from a 3 MV Pelletron accelerator and 2.05-2.85 MeV He^{++} ions, degraded through a rotating aluminum foil, from a 1.7 MeV Tandetron accelerator to simulate damage and transmutation gas, respectively. Experiments were performed to 188, 350, 450, 550 and 650 dpa at 460ºC with a constant helium-to-dpa ratio of ~4 appm He/dpa. The microstructural behavior was examined using both conventional transmission electron microscopy and scanning transmission electron microcopy. The bubble and cavity behavior were examined for each condition to map out the effect of increased damage level on swelling.

A bimodal size distribution was observed at all damage levels indicating the presence of both bubbles and cavities. The average cavity diameter increased with increasing damage level while the number density decreased slightly. The increased diameter was more significant than the decreased density which led to increased swelling with increased damage level. The maximum swelling reached was 6.5% at 650 dpa.

This work is supported by the TerraPower, LLC.

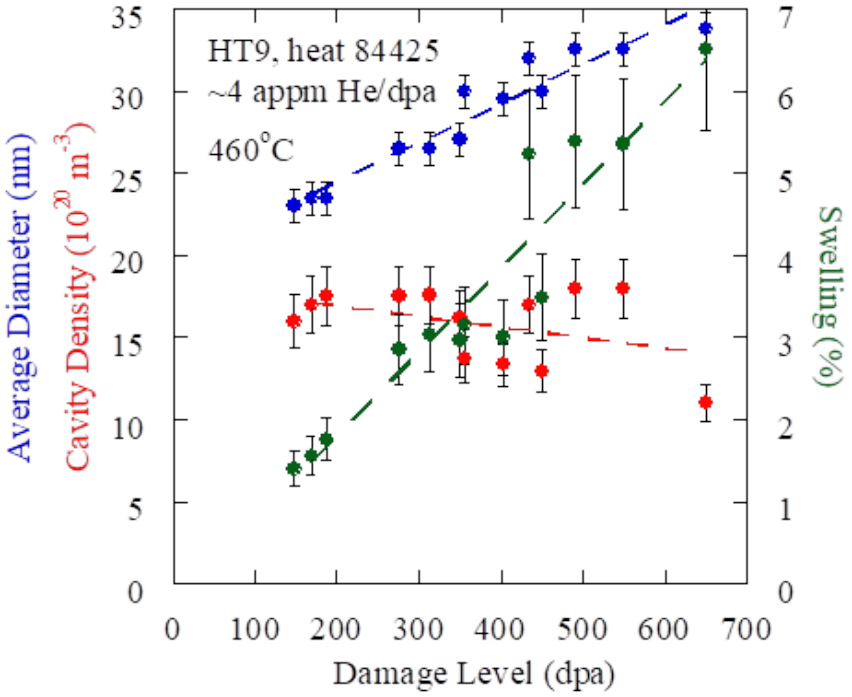

Cavity diameter, density and swelling in HT9 heat 84425 as a function of damage level at 460ºC with a helium-to-dpa ratio of ~4 appm He/dpa. The plot ignores the bubbles and smaller cavities (diameter <10 nm) for all cases. The lines are there to guide the eye and do not represent trend lines.

DEFECT EVOLUTION IN SINGLE AND TRIPLE ION IRRADIATED FeCrAl ALLOYS

P. Xiu[1], L. Jiang[1], C. Ye[1], L. Wang[1,2]
[1]Department of Nuclear Engineering and Radiological Sciences, University of Michigan
[2]Department of Materials Science and Engineering, University of Michigan

FeCrAl alloys are considered as a candidate accident tolerant fuel (ATF) cladding material for light water reactor (LWR) applications. The addition of Cr and Al gives significantly improved oxidation resistance to the alloys so that the material can survive under extreme environments including high temperature and high irradiation dose. The goal of this work is to examine the defect evolution under single and triple beam irradiations.

Figure (a) below shows a FeCrAl alloy irradiated by 6 MeV Au^{++} ions to 100 dpa damage level at 300 nm depth from the surface at 475°C. The on-zone [100] cross-sectional STEM bright-field image in (a) shows the irradiation induced dislocation loops, both plan-view & edge-on <100> loops, which are immobile, and elliptical ½<111> loops, which are mobile. Voids are not observed in single ion irradiated FeCrAl sample showing good swelling resistance of FeCrAl under single ion irradiation. Figure (b) below shows a FeCrAl alloy irradiated by 5 MeV Fe^{++} ions to 50 dpa damage level with the co-implantation of energy-degraded helium of 2.92MeV initial energy (10appm/dpa) and hydrogen of 270 keV (60 appm/dpa) at 475°C. TEM-BF under focus image shows bubbles after the triple beam irradiation. The comparison between them shows that even though the damage level from single beam irradiation is as high as 100dpa, voids were not formed; with the co-implantation of He and H, however, cavities were nucleated at lower damage level of 50dpa. This result shows the role of the gas atoms play in facilitating bubble nucleation and growth, and thus results in swelling in FeCrAl alloys.

The support for this work was provided by CNPRI with the grant #2015ZX06004001.

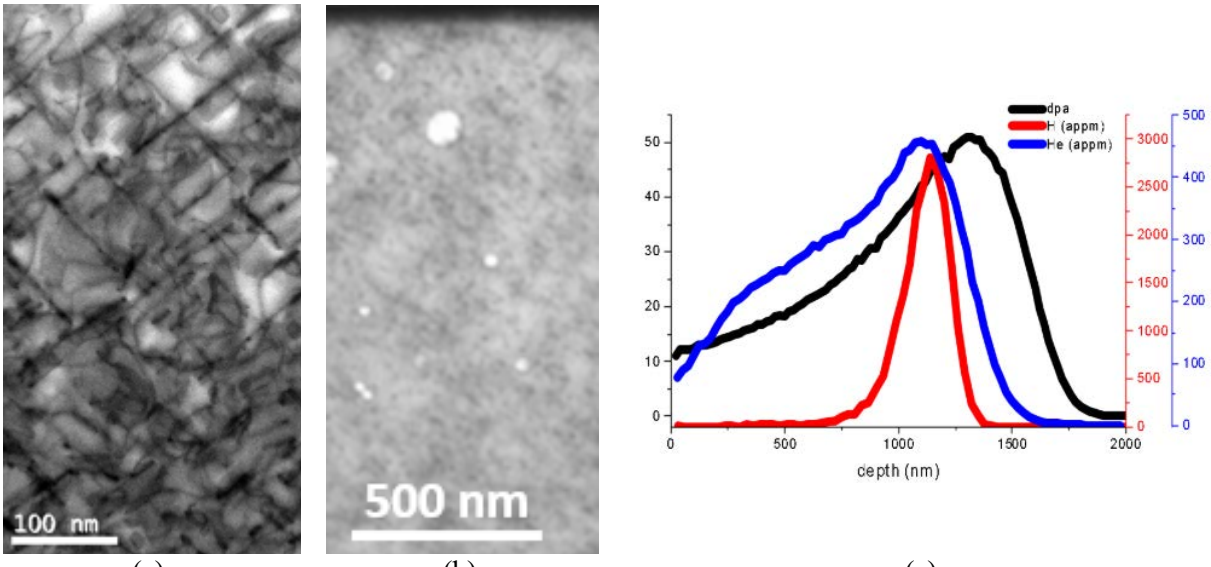

(a) (b) (c)

(a) On-zone [100] cross-sectional STEM bright-field image of FeCrAl after 6MeV Au^{++} irradiation to 100dpa at 475°C; (b) Cross-sectional TEM bright-field image of FeCrAl after 5MeV Fe^{++} irradiation to 50 dpa with co-implantation of H and He at 475°C. (c) SRIM calculation of damage profile (black), with H (red) and He (blue) implantation profile in the triple beam irradiation.

VOID EVOLUTION IN HEAVY ION IRRADIATED MOLYBDENUM ALLOYS AT ELEVATED TEMPERATURES

P. Xiu[1], L. Jiang[1], C. Ye[1], L. Wang[1,2]
[1]Department of Nuclear Engineering and Radiological Sciences, University of Michigan
[2]Department of Materials Science and Engineering, University of Michigan

Molybdenum alloys (Mo) are considered as a candidate cladding material for the accident tolerant fuel (ATF) of light water reactors (LWR) applications because it is a refractory material that has excellent high temperature oxidization resistance, a highly desired property compared to conventional zirconium alloys. The goal of this work is to examine void evolution with increasing irradiation temperatures (900℃-1100℃) simulating accidental reactor condition with high radiation dose and temperature. 6 MeV Au^{++} ions were used to irradiate Mo alloys at 900℃, 1000℃, 1100℃ to reach 100 dpa damage level at 300 nm depth from the surface.

The images below show the irradiated microstructures of a Mo alloy. It can be seen that void swelling becomes more severe as the temperature goes up, indicating that the peak swelling temperature could possibly be even higher than 1100℃ in the Mo alloy. In addition, dislocation loops do not exist in these samples irradiated at high temperatures; instead, only dislocation networks exist in the Mo alloy irradiated at 900℃. At higher temperatures, dislocation networks disappear as a result of temperature enhanced diffusion. Interstitials migrate to either surface, strong defect sinks, or deeper in the sample.

The support for this work was provided by CNPRI with the grant #2015ZX06004001.

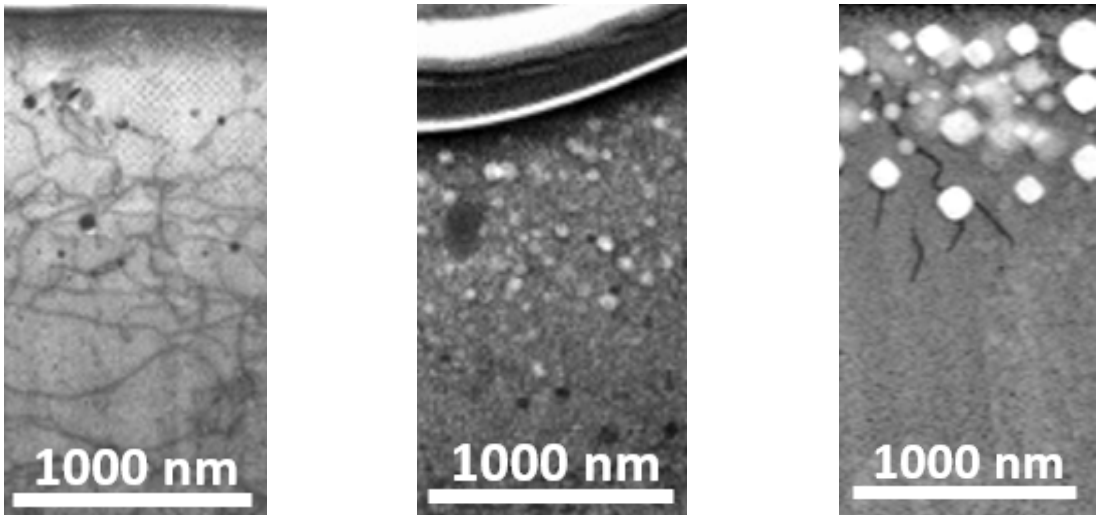

(a) (b) (c)

On-zone [100] cross-sectional STEM bright-field image of Mo alloy after 6MeV gold irradiation to 100 dpa at (a) 900℃ (b) 1000℃ and (c) 1100℃.

IRRADIATION RESPONSES OF COMMERCIAL NI-BASED ALLOYS

L.-J. Yu, E. Marquis
Department of Materials Science and Engineering, University of Michigan

Commercial Ni-based alloys are widely used as structural materials in nuclear power plants due to their superior high-temperature strength and corrosion resistance. However, the limitations associated with neutron irradiation experiments, such as cost, prolonged irradiation time, radioactivity issues, and limited capability of the control of experimental conditions, lead to the paucity of microstructural evolution data in Ni-based alloys. Ion and proton irradiations have been employed to facilitate the study of irradiation effects on materials' microstructures. To further infer the neutron irradiation responses using ion/proton irradiation results, differences between neutron and ion/proton irradiations, such as damage rate, cascade morphology and damage efficiency, and their potential influences on the resulting irradiated microstructures need to be understood. In addition, stability of precipitated phases and defects behavior are strongly dependent on temperature. Therefore, understanding how microstructures change with temperature is beneficial for providing thorough picture of irradiation responses of a specific alloy.

The objective of this study is to investigate the irradiation responses of commercial Ni-based alloys (Alloy 625, Alloy 625 Plus and Alloy 690) under various irradiation conditions (dose, dose rate and temperature). Solution-annealed and aged samples were irradiated at the Michigan Ion Beam Laboratory using 2 MeV protons at the dose rates of ~10^{-5} dpa/s or 5 MeV Ni ions at the dose rates of ~10^{-4} and ~10^{-3} dpa/s, with the dose ranging from 1.5 to 11 dpa at the temperatures of ~300 and ~400 °C. Microstructures including voids, dislocation loops, solute clustering, precipitates and solute segregation, were characterized using transmission electron microscopy (TEM) and atom probe tomography (APT).

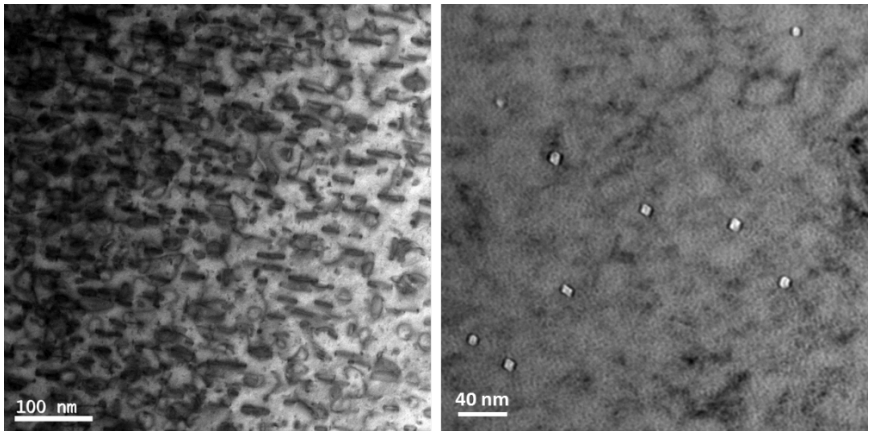

Representative TEM images of dislocations (left) and voids (right) in Alloy 690 after proton irradiation at 300 °C for 6 dpa.

EVOLUTION OF CAVITIES IN A SiC_f/SiC COMPOSITE UNDER TRIPLE ION BEAM IRRADIATION

C. Ye[1,2], J. Xue[3], T. Liu[3], Y. Yan[3], G. Ran[2], K. Sun[4], L. Jiang[2], P. Xiu[2], L.M. Wang[2,4]

[1]College of Energy, Xiamen University, Xiamen, Fujian, China
[2]Department of Nuclear Engineering and Radiological Sciences, University of Michigan
[3]China Nuclear Power Technology Research Institute CO., LTD, Shenzhen, China
[4]Department of Materials Science and Engineering, University of Michigan

Due to its perfect high-temperature stability, creep resistance, excellent irradiation resistance and low neutron capture cross-section, silicon carbide (SiC) is known to be a promising material used as the structural support components in TRISO nuclear fuel and the next generation cladding in accident tolerant fuel (ATF). The goal of the study is to research the evolution of microstructure of a new type of SiCf/SiC composite under simultaneous H, He and Fe ion beam irradiations at 475°C with the peak displacement damage level up to 47 dpa and concentrations of He and H up to 38 and 3400 appm, respectively. Results show that the interface between SiC fiber and PyC interface cracked after the triple ion beam irradiation. The PyC interface could infiltrate into SiC coating to cause deformation of the multilayers due to volume expansion. While no obvious cavities were observed in multilayer SiC coating and SiC matrix, He bubbles as large as 15 nm in diameters were observed at the peak displacement damage region in the SiC fiber and the interface between SiC coating and PyC phase. Helium and hydrogen promote nucleation and growth of cavities by either pressurizing the cavities or reducing their surface energy.

The support for this work was provided by CNPRI with the grant # 2015ZX06004001.

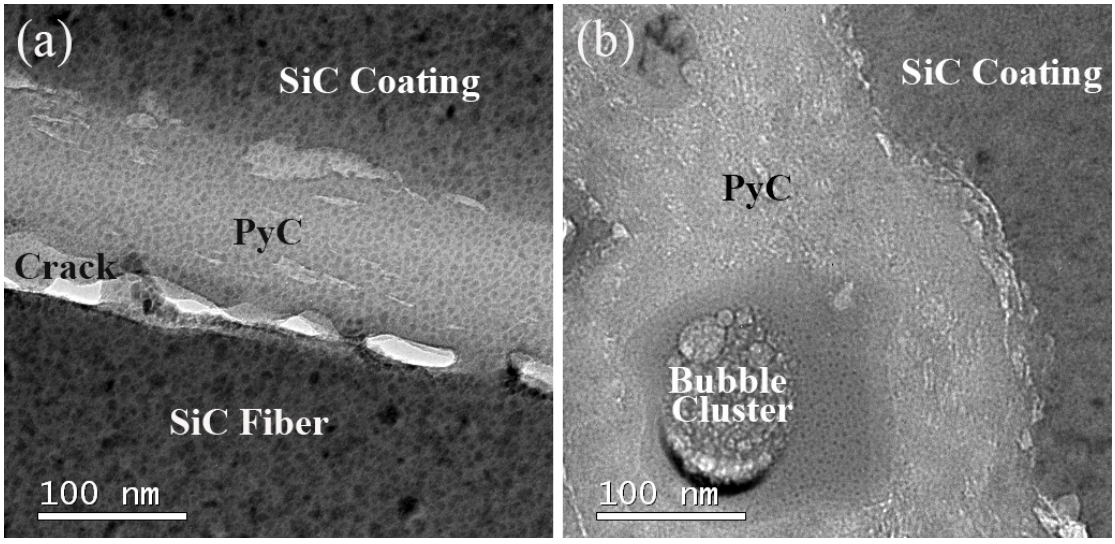

Bright field TEM image of the sample under the irradiation of triple beam, (a) PyC interphase region; (b) The interface between multilayer SiC coating and PyC interphase.

EFFECTS OF MULTI-ION BEAM IRRADIATIONS ON A Cr COATING

L. Jiang[1], P. Xiu[1], L.M. Wang[1,2]
[1]Department of Nuclear Engineering and Radiological Sciences, University of Michigan.
[2]Department of Materials Science & Engineering, University of Michigan.

The goal of this work is to study the effects of hydrogen and helium in a Cr coating over a Zr alloy. The samples were irradiated at 475 ℃ with 5 MeV Fe^{++}, 2.9 MeV He^{++} and 270 keV H^{+} ions under single (Fe^{++}), dual (Fe^{++}+ H^{+} or Fe^{++}+ He^{++}) or triple beam (Fe^{++}+ H^{+} + He^{++}) conditions. The irradiation experiments were performed using the tandem ion accelerators, as well as the 400 kV implanter at the Michigan Ion Beam Laboratory (MIBL). Cavity formation along the depth in all samples was analyzed and compared by cross-sectional TEM focusing on regions around 800 nm in depth where damage dose was 50 dpa with hydrogen-dose ratio of 70 appm/dpa and helium-dose ratio of 12 appm/dpa. Figures below are the HAADF-STEM images from the single, dual and triple ion beam irradiated samples. Results suggest that hydrogen can promote cavity growth and helium can accelerate cavity nucleation. The (Fe^{++} + H^{+}) irradiated sample displays the highest swelling due to the larger cavity size. Dual- or triple-beam irradiations involving He^{++} ions generate lower swelling because of the smaller cavity size despite of the high cavity density.

The support for this work was provided by CNPRI with the grant #2015ZX06004001.

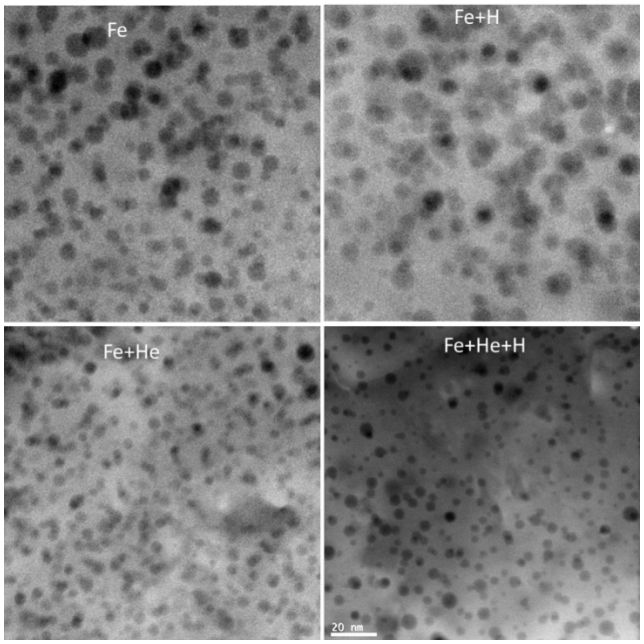

HAADF-TEM images showing the cavity characteristics of the Cr coating after irradiated with (a) Fe^{++}, (b) Fe^{++} + H^{+}, (c) Fe^{++} + He^{++}, (d) Fe^{++} + H^{+} + He^{++}.

PLANAR ION CHANNELING STUDIES OF GaN SURFACES

J. He, G. Cheng, D. DelGaudio, J. Occena, F. Naab*, and R.S. Goldman
Dept. of Materials Science & Engineering, *Michigan Ion Beam Laboratory, U-Michigan
M. Nami, B. Li, and J. Han
Department of Electrical Engineering, Yale University

Although silicon-based electronics are used for light-emitting diodes and electric vehicles, their utility in high power applications is limited by a low breakdown voltage. A promising alternative is vertical GaN devices, but these require regrown active regions which require special chemical treatments. Therefore, we are examining the influence of various chemical treatments on the structure of GaN surfaces. Using the new fully-automated 5-axis goniometer, we have performed Rutherford Backscattering spectroscopy with a 1.5 MeV H ions to visualize the distribution of displaced Ga atoms near the surfaces. Here, we present planar ion channeling maps (Fig. 1) and angular yield profiles (Fig. 2) of (a) as-received and (b) tertiary-butyl-chloride (TBCl)-etched GaN surfaces. The greater asymmetry of the angular yield profile for the TBCl-etched GaN indicates a higher fraction of displaced Ga atoms in that case.

This work is supported by ARPA-E AED0000191 and the Michigan Ion Beam Laboratory.

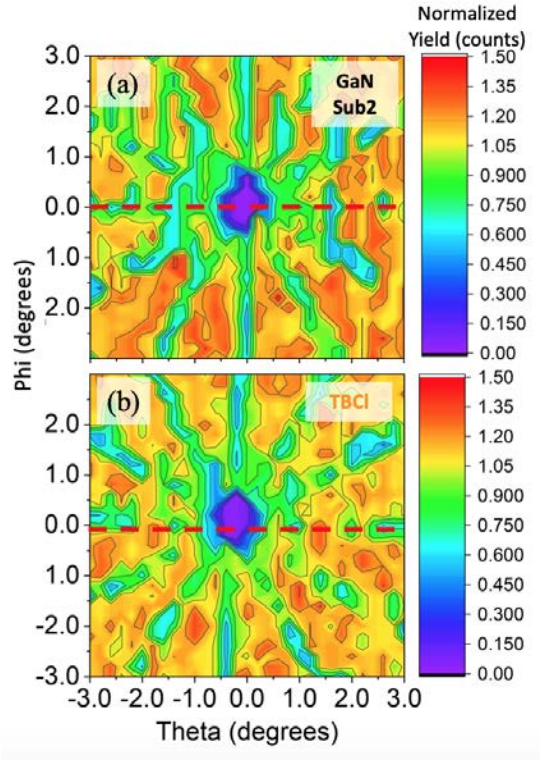

Figure 1. Normalized planar ion channeling maps about the [0001] axis for (top) as-received and (bottom) tertiary-butyl-chloride-etched GaN surfaces. The channels were identified by rotating the goniometer in steps of 0.2° in theta and phi. The normalized yield is integrated over channels 820-845 (corresponding to a depth of ~370nm).

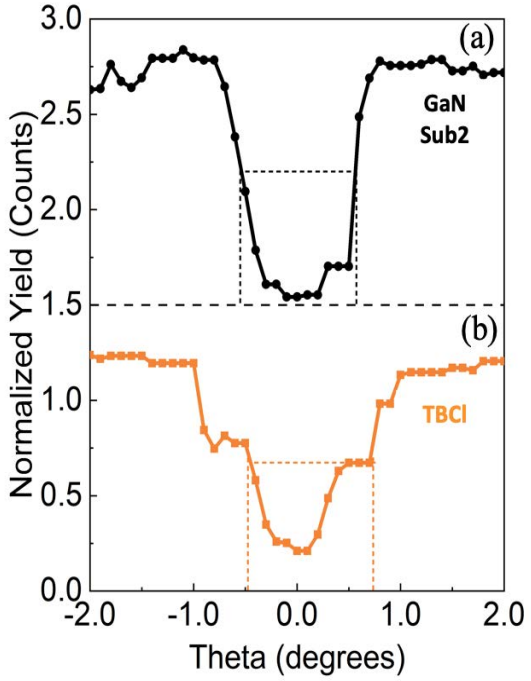

Figure 2. Angular yield profiles (red dashed horizontal lines in Fig. 1) collected in the (11-20) plane about the [0001] axis for the (a) as-received and (b) tertiary-butyl-chloride (TBCl)-etched GaN surfaces. The greater asymmetry of the angular yield profile for the TBCl-etched GaN surface indicates a higher fraction of displaced Ga atoms in that case.

STRONG ENHANCEMENT OF THz EMISSION IN A METAL-GRAPHENE-SILICON HETEROSTRUCTURE

D. Zhang, Z. Xu, G. Cheng, Z. Liu, A.R. Gutierrez, T.B. Norris, Z. Zhong
Department of Electrical Engineering and Computer Science, University of Michigan

Photoconductive antennas are an important technology for THz pulse emission. It enables a wide range of applications in THz imaging and time-domain spectroscopy. Significant efforts have been made ?? by many groups to streamline the performance metrics, including the optical power conversion efficiency, bandwidth, optical saturation, signal-noise ratio (SNR) and operation at different pump wavelengths. Previous works have reported greatly enhanced THz emission using antenna designs with interdigitated electrodes and plasmonic nanostructures. However, these solutions require very small feature sizes and correspondingly increased fabrication complexity. Here we report a novel alternative strategy to enhance the THz emission: with insertion of a graphene layer, the THz signal emitted can be dramatically increased in a silicon Auston switch. We used an on-chip pump-probe measurement to study the device (Fig (a)). Observations indicate that the graphene layer, with its high carrier mobility, works as a very efficient channel for the photogenerated hot carriers in silicon to be extracted by the metal contacts. This leads to a 10-to-80-time enhancement of THz emission. The work unveils a new strategy to build strong THz emitters with simple structures. We believe that further understanding of the system will lead to low cost, strong THz emitters for imaging and spectroscopic applications.
As shown in Fig. (a), the device was fabricated on a silicon-on-sapphire substrate, with a silicon thickness of 300 nm. The silicon was first implanted with O^+ ions. The ion-induced defects work as recombination centers, reducing the hot carrier relaxation time to 0.7 ps. A CVD-grown graphene layer is then wet-transferred to the substrate. It is then patterned into a graphene channel using photolithography and oxygen plasma etching. Finally, a 300-nm-thick layer of gold is deposited onto the sample as metal contacts and double-stripe THz waveguides.

During our measurement, a bias is applied across the graphene channel. A pump laser pulse illuminates the metal-graphene-silicon heterostructure, generating a THz field that is coupled to a coplanar waveguide, then measured by an Auston switch. The pump generates a large population of hot carriers in the silicon. In a simple Auston switch structure with no graphene layer, the electric field in the gap only collects hot carriers generated very close to the contact, limiting the amplitude of THz signal emitted. In our structure, the graphene layer has a much higher mobility than the highly defective silicon, enabling charges to be collected over a much larger region and transported to the contacts. We observe an 80x enhancement of field amplitude, with no tradeoff of bandwidth or SNR.

The authors gratefully acknowledge financial support from the National Science Foundation (ECCS-1509354). Devices were fabricated in the Lurie Nanofabrication Facility and the Michigan Ion Beam Laboratory (MIBL) at University of Michigan.

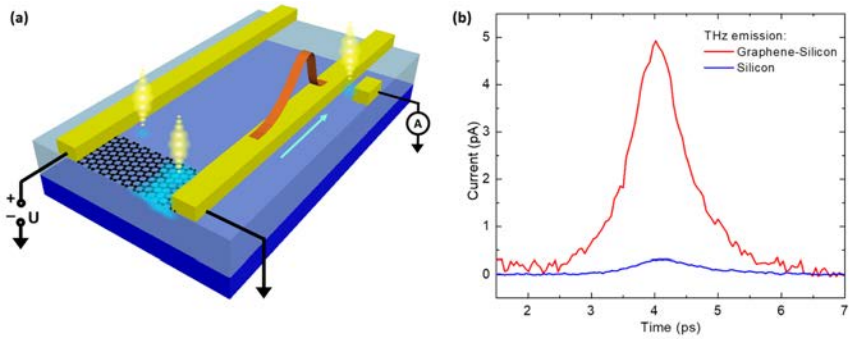

(a) Schematic of the THz emitter based on metal-graphene-silicon heterostructure. A transmission line is used to couple the field to an Auston switch (detector). (b) Giant enhancement of THz emission, the bias is 6V, with pump power of 3 mW and probe power of 10 mW for both emitters.

PROBING THE EFFECT OF SI ION-IMPLANT IN ENHANCING THE CHARGE TRANSPORT ACROSS METAL-SEMICONDUCTOR JUNCTIONS FOR EMERGING Ga_2O_3 SYSTEM

M.-H. Lee[1], R.L. Peterson[1, 2]
[1]Department of Materials Science and Engineering, University of Michigan
[2]Department of Electrical Engineering and Computer Science, University of Michigan

To achieve the full potential of high-power, high-frequency Ga_2O_3 power devices, a low-resistance ohmic contact is necessary to minimize conduction loss. The objective of this study is to enhance the ohmic property (i.e. to minimize the contact resistance) via ion-implantation. To engineer the ohmic contact, one of the well-known methods is to degenerately dope the semiconductor to enable tunneling across the junction. Based on theoretical works and previous reports, we know that in Ga_2O_3, silicon acts as a shallow donor, increasing the free carrier concentration. Therefore, we choose Si ion implantation to form a heavily doped layer at the β-Ga_2O_3 surface.

We implant the Si ions using multiple implants with different energy and dose conditions to achieve a total fluence of 10^{15} ions/cm^2 with a ~180 nm Si implant box profile. A post-implant activation anneal was carried out at > 900°C in N_2 environment to recover implant-induced crystalline damage and to activate the Si atoms as shallow donors. Afterward, device fabrication was done with conventional a photolithography and lift-out process to pattern evaporated Ti/Au metallization with Circular Transmission Line Model (CTLM) structures. A post-metallization anneal was carried out at 470°C N_2 for 1-min to further improve the ohmic properties. For comparison, devices with same process were made on another un-implanted sample.

Without ion implant, the specific contact resistivity is measured to be 3.29×10^{-3} Ω·cm^{-2} at room temperature, whereas, on the implanted sample the specific contact resistivity is reduced to 1.51×10^{-4} Ω·cm^{-2} at room temperature. The reduction in contact resistance observed with silicon ion implant is attributed to the heavily-doped layer, which facilitates charge transport. To further investigate the transport mechanisms, temperature-dependent current-voltage characteristics are measured. For both of the samples, increasing the temperature reduces the specific contact resistivity. The electrical behavior of the implanted and non-implanted samples can be described by thermionic-field emission (TFE) and thermionic emission (TE) model, respectively. Results from this study pave the way for realizing and optimizing high-quality contacts for next generation Ga_2O_3 power electronics.

CALIBRATION OF A SPUTTER SYSTEM FOR PHOTOCATHODE FABRICATION

A. R. Ansari[1], A. Sarracino[1], B. Torralva[2], S. M. Yalisove[1,3]
[1]Department of Applied Physics, University of Michigan
[2]Department of Climate and Space Sciences, University of Michigan
[3]Department of Materials Science and Engineering, University of Michigan

The performance of a photocathode is measured by the photoelectron yield that is observed. Gold (Au) is a common material for use as the active material in photocathodes due to its stability in air, resistance of contaminants, and high current density yields. The thickness of the Au film must be tightly controlled to allow for electron transmission. When irradiating Au films with an ultrafast pulse inside an extracting electric field, Au films on silica substrates ruptured after repeated irradiation. This was attributed to poor bonding between Au and the oxide. To improve Au adhesion, a thin film of a different species, such as titanium (Ti) or tungsten (W), can be used as an adhesive layer, since these species bind much more strongly to silica. This means that the W layer must be thin enough to allow sufficient light transmission for photoelectron generation in the Au while still providing sufficient adhesion. The thickness of both metals, therefore, must be controlled precisely. To control the thickness of sputtered films, the deposition rate for given working conditions must be determined. Calibrating the deposition rate to sub-nanometer accuracy requires a measuring technique of high sensitivity and low noise. Rutherford Backscattering Spectrometry (RBS), a technique with low relative uncertainty, was used to measure the thickness of the films.

On fuse silica substrates, films of Ti and films of Au on a thin layer of Ti were deposited with varying deposition times. A 2 MeV beam of helium ions was then incident on the surface of these films. A detector at an angle of 165° relative to the incoming beam was used to collect the scattered ions. After the data was collected, SIMNRA was used to model and perform a fit to extract the thickness of the films. Features from the substrate, fused silica, were observed. A deposition rate of 0.119 nm/s was calculated for Ti and 0.805 nm/s was calculated for Au.

This work is sponsored by the Air Force Office of Scientific Research Contract Number FA9550-16-1-0312.

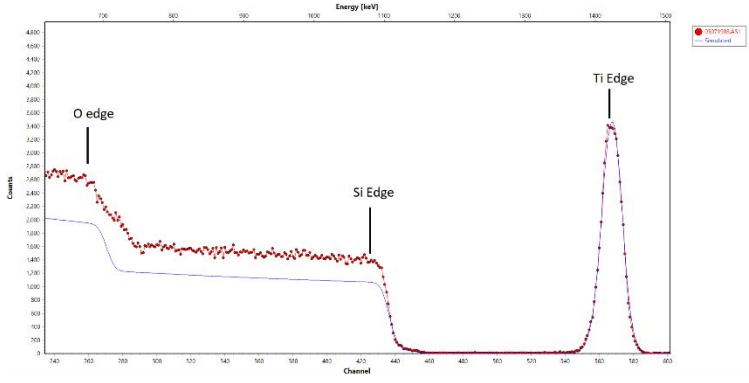

An RBS spectrum with an accompanying fit obtained from SIMNRA. The thickness of the Ti film on fused silica was extracted. This peak corresponded to a thickness of 38.70 nm.

The thickness values extracted from the RBS spectra for two films each of Ti and Au, each with different deposition times.

Metal	Time (s)	Thickness (nm)
Ti	66.7	7.0356
	333.3	38.6958
Au	13.2	8.469
	65.8	50.814

RESPONSE OF SCINTILLATOR TO LOW ENERGY PROTONS

D. Levin, C. Ferretti, N. Ristow, P. Friedman*
Dept of Physics, University of Michigan
*Integrated Sensors, LLC, Toledo, OH

The primary objective of this study was measurement of the light yield from a thin plastic proprietary scintillator. The specific objectives were to image the beam using this particular scintillator, and to measure its response to energy loss and derive Birks saturation parameter.

For this purpose, a small 2 cm x 2 cm scintillator sample was mounted on a pedestal at the back cover flange of the beam line. Scintillation light was recorded using a Basler CMOS sensor camera mounted on a viewport at 12 inches from the specimen. The beam current was set to a nominal 1 nA, and recorded before and after each data run. The beam currents were dumped to log files for later use. Data were taken with beam energies ranging from 5.4 to 4.5 MeV. For each energy step, the same scintillator sample was used. Exposures were for 20 seconds, with data acquired also before and after the beam was enabled. These before/after data were used to extract the ADC pedestals, and to also establish the average beam current during the run. The beam currents were used to normalize all ADC measurements.

The basic analysis method includes selection of a fiducial region of the scintillator from which an average ADC value (which represents the light yield) was determined. These average ADCs were then renormalized to an equivalent current. For each beam energy a proton energy loss in the scintillator was calculated using online PSTAR tables.

Results: This study was successful, but the final result is somewhat degraded by the instability of the beam current, which varied from 5% to 8% over the course of a series of runs. Preliminary analysis of the data has been completed and the results are proprietary and currently unpublished. An additional measurement is anticipated in 2020 using a higher and more stable beam current.

This work was supported by the U.S. Department of Energy, Office of Nuclear Energy Phase 1 SBIR contract: DE-SC00195597

ION IRRADIATION INDUCED ALPHA PRIME PRECIPITATE FORMATION OR DISSOLUTION IN IN HIGH PURITY Fe-Cr ALLOYS

Y. Zhao[1], A. Bhattacharya[2], S.J. Zinkle[1,2,3]
[1]Material Science and Engineering Department, the University of Tennessee
[2]Materials Science and Technology Division, Oak Ridge National Laboratory
[3]Nuclear Engineering Department, the University of Tennessee

Binary Fe-Cr alloys are simple representatives of ferritic-martensitic steels which are structural material candidates for Gen. IV fission and fusion reactors. For Cr levels >8-9% and irradiation temperatures below ~480°C, these alloys suffer from neutron irradiation-induced/enhanced embrittlement due to Cr-rich α' precipitation. The formation of α'precipitates has been reported in literature after neutron, electron and low dose rate ion irradiations. However, there is still a gap between the very recent results and previous results in which α' clusters were absent after ion irradiation. To bridge this gap, we decreased the irradiation temperature and increased the dose rate compared to our earlier work to gradually approach the conditions conventionally used to test the ion irradiation behavior of FeCr alloys (about 300°C – $1x10^{-3}$ dpa/s), so that the critical condition for the α' precipitates to form or dissolve can be obtained.

Four irradiation conditions were selected at temperatures of 350 - 450°C up to mid-range doses of 0.35 dpa, with dose rates 10^{-4} -10^{-3} dpa/s, and all of the experiments have been completed. Thin (300 - 400 μm) disks of 3 mm diameter for Fe-(10-18 at. %)Cr samples were prepared. All of the experiments were requested to use 8 MeV Fe ions. The figure (a) below shows the damage profile, in which total doses of 0.35 displacements per atom (dpa) at 1μm depth was collected. Temperature alignment was done through thermocouples, spot-welded on to the Fe-12Cr disks, and it was monitored by infrared camera through the whole irradiation. Pressure and beam currents were recorded during the irradiation experiments. An example of sample arrangement on the stage is given in Figure (b). Comprehensive characterization of the sample microstructures is in progress.

This work was supported by the Office of Fusion Energy Sciences, U.S. Department of Energy (grant # DE-SC0006661 with the University of Tennessee and contract DE-AC05-00OR22725 with UT-Battelle, LLC).

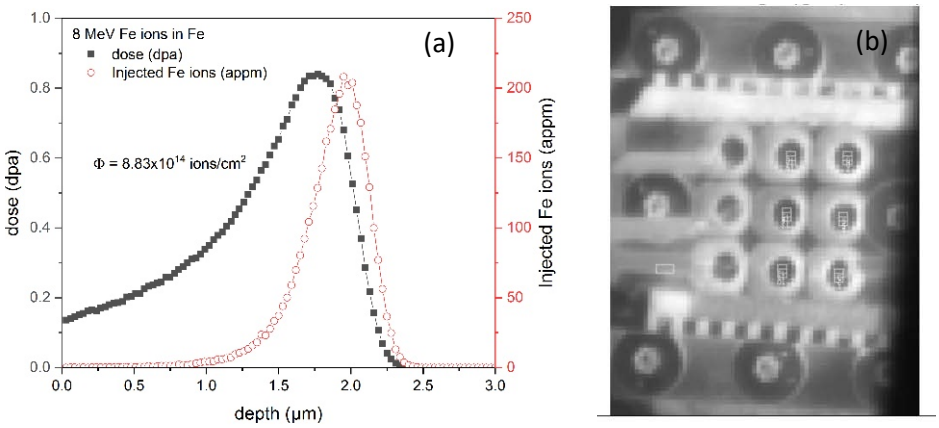

(a) SRIM based estimates of depth profile of displacement damage in dpa and implanted Fe ions concentration in pure Fe. (b) An example of sample arrangement on the stage.

STUDY OF THE VOID SWELLING IN ION IRRADIATED HIGH-PURITY Fe AND Fe-Cr ALLOYS

Y.-R Lin[1], A. Bhattacharya[2], J. Henry[3], S.J. Zinkle[1,2*]
[1]University of Tennessee, Knoxville
[2]Oak Ridge National Laboratory, Oak Ridge, TN
[3]CEA, DEN-Service de Recherches Métallurgiques Appliquées, Laboratoire d'Analyse Microstructurale des Matériaux, Université Paris-Saclay, F-91191, Gif-sur-Yvette, France

Reduced activation ferritic and ferritic/martensitic (FM) steels containing 8-12%Cr are promising structural material candidates for fusion and advanced fission reactors due to their attractive mechanical properties and volumetric swelling resistance. Experimental studies of irradiated Fe–Cr alloys have reported void swelling suppression by the addition of Cr to the Fe matrix. However, significant discrepancies have been reported regarding the temperature dependence of void-swelling (temperature range and peak swelling temperatures) under ion versus neutron irradiation conditions. In particular, some studies have reported a much narrower range of temperatures for observable void swelling in ion irradiated samples (which may be partially affected by implanted ion and/or near-by surface effects). In addition, He synergistic effects and the effect of impurity additions that are commonly known to interact with vacancies (like C, N, O) are not yet clearly quantified. In this context, we have performed multi-temperature (400, 435, 470, 500, 550°C) simultaneous dual beam ion irradiations (using 8 MeV Ni^{3+} ions and energy-degraded 3.5 MeV He^{2+} ions) on a series of ultra-high purity bcc Fe and Fe-Cr alloys with Cr content ranging from 3-14% Cr and a Fe-10%Cr alloy with 760 ppm C. A heavy ion energy of 8 MeV (2.5 μm range) was selected to provide a relatively wide mid-range region (~0.5-1.5 μm) for quantitative analysis that is not affected by near-surface or implanted ion effects. Mid-range (1.0 μm) irradiation conditions were 30 dpa, 0.1 appm He/dpa, 1.4×10^{-3} dpa/s. Using state-of-art transmission electron microscopy (TEM), scanning TEM (STEM) and comparing with published neutron irradiated results, we revealed that Fe has a ~50 °C lower peak swelling temperature than Fe-Cr alloys. Additionally, Cr suppressed void swelling of ion irradiated Fe-Cr alloys below ~470°C, but enhanced swelling above ~470°C. By comparing the results in Fe10%Cr with and without C, we found that the addition of carbon for Fe-10Cr at temperatures below 550°C tends to decrease the swelling.

This research was sponsored by the Office of Fusion Energy Sciences, U.S. Department of Energy under contract DE-AC05-00OR22725 with UT-Battelle, LLC and grant # DE-SC0006661 with the University of Tennessee. The ultra-high purity Fe and Fe-Cr samples were supplied by the EUROfusion consortium.

ROLE OF GRAIN BOUNDARY SOLUTE SEGREGATION ON GRAIN BOUNDARY COHESION

P.H. Warren, J.P. Wharry
School of Nuclear Engineering, Purdue University

The objective of this study is to understand the role of solutes in grain boundary cohesion. Intergranular fracture, specifically, is associated with solute segregation to grain boundaries (GBs), which is believed to increase the GB surface energy and decrease the GB cohesive energy, culminating in GB decohesion or cleavage. But there is mounting theoretical evidence GB separation is not attributed to simple bond-breaking arguments, but rather to the inhibition of dislocation nucleation. Recent advancements in transmission electron microscopic (TEM) in situ mechanical testing now enable verification of these theories through the direct observation of crack propagation at sub-nanometer resolution. In this project, ion irradiation is used as a tool to intentionally produce GB segregation of solute species. Specifically 4.5 MeV Fe^{2+} self-ion irradiation at 350°C is conducted on model Fe-based binary alloys containing additions of Cr, Mo, Mn, P, or N. An irradiation dose of 10 displacements per atom (dpa) is attained at a depth of 500 nm, calculated by the Kinchin-Pease model using SRIM 2013.

Following ion irradiation, TEM in situ tensile testing will be conducted on specified grain boundaries (e.g. Σ3, Σ7, random high angle boundary). Thus far, work has focused on the development of the TEM in situ method. The specimen preparation by focused ion beam (FIB) milling has been refined, and test cases on as-received (unirradiated) Fe-5at%Mo have been carried out. The TEM in situ tensile tests reveal a dramatic decrease in local dislocation density in the vicinity of the fracture, immediately preceding the fracture (see circled region in figure). In the coming months, irradiated specimens will be studied, and irradiation-induced changes in fracture mechanism will be identified.

This work was supported by the National Science Foundation CAREER award DMR-1752636.

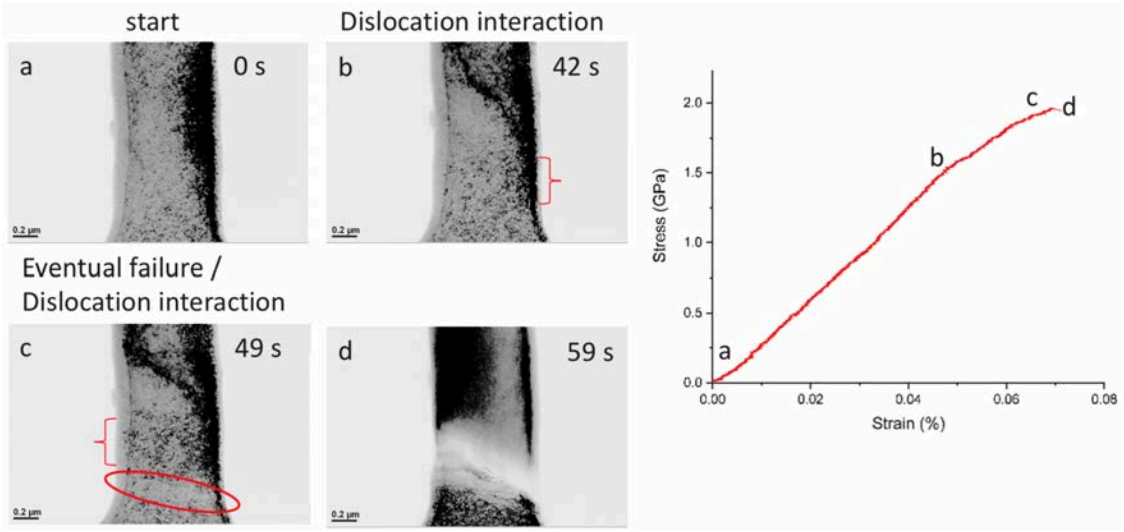

Still frame images from TEM in situ tensile test of as-received Fe-5at%Mo, revealing localized reduction in dislocation density in the vicinity of the fracture, immediately preceding the fracture (circled); stress-strain curve is marked at points corresponding to the still frames shown.

SELF-ORGANIZATION OF Kr GAS BUBBLE SUPERLATTICE IN METALS UNDER ION IMPLANTATION

C. Sun, J. Gan
Idaho National Laboratory, Idaho Falls, ID 83415

The objective of this proposal is to study the physical mechanisms of krypton gas bubble superlattice (GBS) in materials by using ion implantation. Under irradiation, the formation of gas bubbles leads to a microstructural evolution where gas bubbles usually cause hardening and embrittlement, degrading the mechanical properties of fuels and materials. Managing the gas bubble formation and transforming them from a liability into an asset in a controllable way will help us tailor the microstructure of nuclear materials and precisely predict the materials performance in nuclear reactors. GBS has been observed for decades, they can form either by gas ion implantation or by nuclear transmutation. Although many possible GBS formation mechanisms have been proposed previously, a clear understanding is still missing. The self-organization of gas bubbles typically form adopts the same structure as the matrix crystal structure. As seen in Figure 1 (a-c), we previously performed helium ion implantation in tungsten at 650˚C, GBS was formed in the materials and exhibit a bcc structure with the same crystal orientation with the host materials. Both selected area diffraction and synchrotron-based small angle x-ray scattering (SAXS) confirms the formation of GBS and the bcc structure. Interestingly, Gan et al. recently reported that fission gas bubbles (Kr and Xe) form an fcc superlattice in a bcc uranium-molybdenum alloy under neutron irradiation. Hu et al. believe that fast 1-D migration of interstitials along <110> directions in the bcc U-Mo matrix causes the gas bubble alignment along <110> directions. Here we create Kr gas bubble superlattice in Mo by using ion implantation and study the role of anisotropy on the formation of heavy gas bubble superlattice. We performed Kr ion implantation in Mo with various implantation conditions, as seen in the table. Rhenium tends to form mixed-interstitial, changing the interstitial diffusion from 1D in pure W to 3D in W-Re alloys. We hypothesize that the addition of Re could prevent the formation of GBS. To test this hypothesis, we performed Kr ion implantation in W, W-3Re, W-6Re and W-10Re. Fundamental understanding of GBS formation in materials under irradiation supports the development of advanced nuclear fuels and materials.

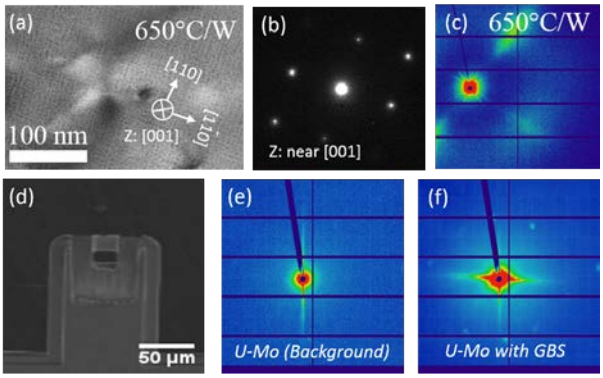

(a-c) Helium gas bubble superlattice in tungsten irradiated at 650˚C. Bright field TEM image (a), selected area diffraction (b) and synchrotron-based small angle x-ray diffraction (c) shows the formation of GBS and the bcc structure of GBS. (d-f) Xe/Kr gas bubble superlattice in U-7Mo alloy after neutron irradiation.

Batch	ID	Sample	Temperature (°C)	Kr energy (keV)	Ion fluence (ions/cm^2)	Flux (ions/cm^2/s)
1	M43-15	Mo	400	300	1.5×10^{16} (3 at.%)	3.8×10^{12}
2	M43-25		400		2.5×10^{16}(5 at.%)	
3	M43-45		400		4.5×10^{16}(9 at.%)	
4	M43-100		400		1×10^{17} (20 at.%)	
5	M33-15		300		1.5×10^{16} (3 at.%)	
6	M33-25		300		2.5×10^{16}(5 at.%)	
7	M33-45		300		4.5×10^{16}(9 at.%)	
8	M33-100		300		1×10^{17} (20 at.%)	
9	W53-25	W	500		2.5×10^{16}	
	W3R53-25	W-3Re				
	W6R53-25	W-6Re				
	W10R53-25	W-10Re				

This work This work was sponsored by the U.S. Department of Energy (DOE), Office of Science, Basic Energy & Science (BES), Materials Sciences and Engineering Division under FWP #C000-14-003 at Idaho National Laboratory operated by Battelle Energy Alliance (BEA) under contract DE-AC07-05ID14517. We also acknowledge the U.S. DOE, Office of Nuclear Energy Nuclear Science User Facility (NSUF) under contract DE-AC07-051D14517

FABRICATION OF THIN-FILM LITHIUM NIOBATE ON INSULATOR THROUGH ION-SLICING

K. Prabhakar, J.T. Nagy, R.M. Reano
Electroscience Laboratory, Department of Electrical and Computer Engineering,
The Ohio State University

In the field of integrated optics, waveguide devices widely utilize ferroelectric materials like lithium niobate (LN) due to its strong nonlinear susceptibility and high electro-optic coefficient. Thin films of LN less than a micron thick are particularly useful for waveguide devices as the mode effective area is further reduced leading to enhanced material properties, making effects like $\chi^{(2)}$ nonlinearity observable even at low optical power levels. LN thin films are usually bonded to an insulating material with a lower refractive index than LN such as silicon dioxide which helps confine the optical power in the lithium niobate thin film. This layer structure is often referred to as lithium niobate on insulator (LNOI). In our project we utilize the ion-slicing mechanism to fabricate LN thin films bonded to thermally oxidized Si wafers.

Magnesium oxide doped LN wafers are implanted with He^+ ions at energies of 130keV and 225keV which leads to the formation of damage layers under the surface of the substrate at depths of 510nm and 750nm respectively as predicted by TRIM simulations. The implanted surface of the LN wafer is then bonded to a thermally oxidized Si carrier and annealed. Heating causes blistering at the site of implantation, and at high enough temperatures layer splitting occurs leaving a wafer-scale LN thin film bonded to the carrier. Wafers implanted at MIBL will undergo subsequent bonding and film exfoliation before finally being polished to achieve sub-nanometer RMS surface roughness values. These films will be used in fabrication of integrated waveguide devices. Additional implantations at MIBL are planned for this project.

This research is supported by the National Science Foundation under Award No. 1809894

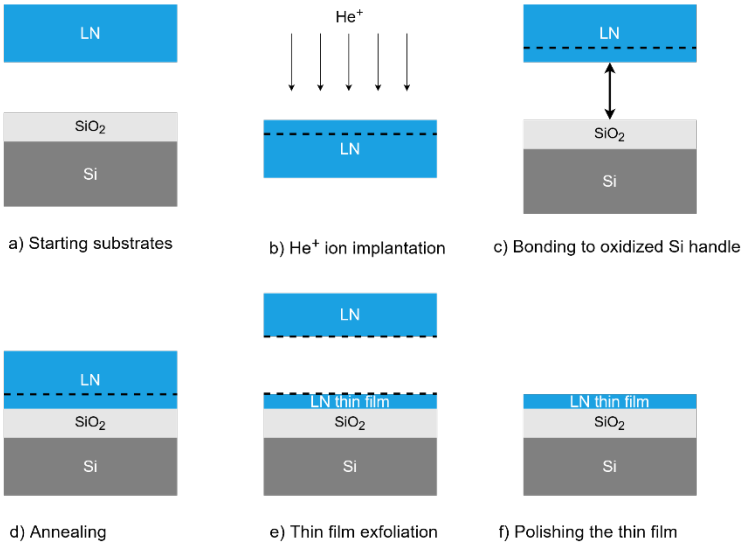

Figure 1. Starting with a 3-inch LN wafer and an oxidized Si substrate (a), the LN wafer is implanted with He^+ ions (b) and bonded to the Si handle (c). The stack is subsequently annealed (d) which leads to a thin film being exfoliated (e). The sample is finally polished (f).

Figure 2. LN wafer temporarily bonded to an aluminum carrier via silver paste inside the implantation chamber.

MICROSTRUCTURAL ANALYSIS TO EVALUATE THE POTENTIAL OF ION IMPLANTATION AS ALTERNATIVE DOPING TECHNIQUE FOR SRF CAVITIES

M. Martinello
Fermi National Accelerator Laboratory

Nitrogen implanted samples were studies in order to understand the potential of ion implantation as a possible alternative to vapor diffusion doping of superconducting RF (SRF) niobium cavities.

The dependency between the ion implantation parameters (dose and energy), the dopant concentration profiles and the damage in the sample was analyzed through different materials characterization analysis and simulation software including SRIM, EBSD, HR EBSD and SIMS analysis. From the SRIM simulation it was found that ion implantation results in a Gaussian shaped depth profile. The shape of this curve can be tuned by variation of the ion energy and dose. Particularly, it was found that higher energy ions penetrate deeper into the material (larger projected range) and distribute over a larger volume (larger straggle). On the other hand, implantation with higher ions doses was found to increase the N concentration and thus shifts the bell-shaped N concentration profile upwards.

Results of the SIMS analysis showed good consistency with the simulation outputs, even though the N concentration depth profiles resulted in a more complicated shape compared to the theoretical Gaussian shape. This was attributed to atypical surface preparation of the samples used for this analysis. Usually Nb samples are electro-polished (EP'ed) as done for SRF cavities, in order to obtain a smooth surface. In this case the samples were buffer chemical polished (BCP) instead, which results in a much rougher surface, which lead to irregular results.

High-resolution electron backscatter diffraction (HR-EBSD) was performed on the cross-section of the samples, in order to analyze the amount of lattice damage due to implantation under different conditions. This analysis concluded that the four samples showed low level of damage in the subgrain structure of the near implanted surface region. This was demonstrated by the absence of fluctuation in the misorientation angle (calculated with both EBSD and HR-EBSD analysis) in correspondence with the vacancy concentration peak (predicted using SRIM simulation). Based on this, the conclusion of the study is that ion implantation do not lead to significant lattice damage and therefore it may be a suitable technique to doped SRF cavities and improve their performance.

STUDY OF CATION DISORDER AFFECTING ELECTRICAL TRANSPORT IN AMORPHOUS OXIDES

S. Husein[1], J. Perkins[2], J. Medvedeva[3], M. Bertoni[1]
[1]Ira A. Fulton Schools of Engineering, Arizona State University
[2]National Renewable Energy Laboratory, Golden, CO
[3]Department of Physics, Missouri University of Science and Technology

In this study, we used a combinatorial sputtering approach for deposition of zinc tin oxide (ZTO) spanning 100% SnO_2 to 100% ZnO with compositional libraries containing a large set of varied Zn:Sn ratio, sputtered at 300 ºC, 400 ºC, and 450 ºC substrate temperatures (T_s). Compositional information and film density were obtained through collaboration with facilities at the Michigan Ion Beam Laboratory.

The as-deposited films grown at T_s = 300 °C exhibit a clear transition from crystalline to amorphous at approximately 37 % [Zn]/([Zn]+[Sn]), revealed by x-ray diffraction. For T_s = 400 °C, a similar transition occurs at 45%. For both T_s, a transition from amorphous to crystalline exists near 70 % [Zn]/([Zn]+[Sn]). Films grown at T_s = 450º C are currently under evaluation. The electrical properties, obtained by Hall effect at room temperature, of the amorphous phase films are of particular interest, and a significant peak in conductivity is observed near the transition from amorphous to crystalline at the three T_s.

While intermediate compounds consisting of $ZnSnO_3$ and Zn_2SnO_4 have been reported [6-8], a complete exploration of the ZnO-SnO2 tie-line and the resulting amorphous phases is lacking. Evaluation of the compositional characteristics of the amorphous phases was carried out by Rutherford backscattering, with oxygen content and film density shown in the figure.

This composition information, and in particular the changing oxygen stoichiometry of the films with increasing Zn%, was used to inform *ab initio* molecular dynamics liquid-quench and density functional theory simulations. Simulations of the amorphous ZTO structures were created using a quench rate of 200 K/ps. By inspecting the coordination of each cation species, it is readily seen that the Zn-O coordination varies significantly compared to Sn-O coordination. More in-depth analysis revealing the coordination of the cation species with varied cation ratio, the number of face, edge, and corner-sharing metal-oxygen polyhedra, and the metal species contribution to the Bader charge near the Fermi energy level are in preparation for publication. However, findings reveal two crucial factors: (1) zinc cations control the morphology and crystallization of the system, which determines the carrier mobility; whereas (2) tin cations govern the carrier generation in the system.

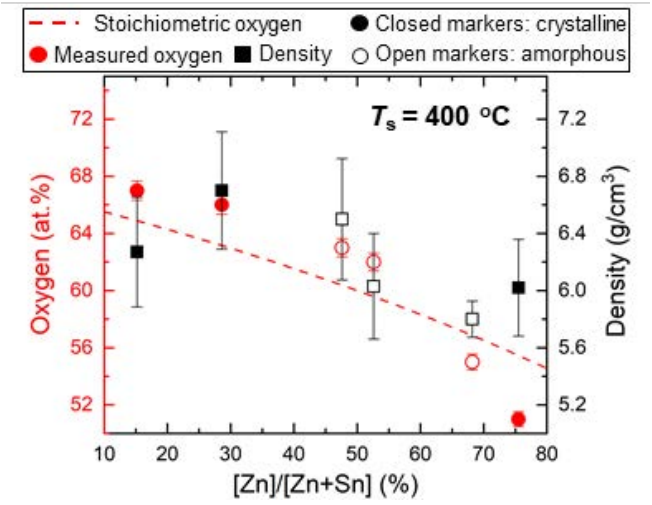

Oxygen content (red circles) and film densities (black squares) measured by Rutherford backscattering of zinc-tin oxide films grown at 400ºC. Closed markers indicate the films are partially crystalline, while open markers indicate the films are fully x-ray amorphous. The dashed, red line is the calculated stoichiometric oxygen atomic % for a given [Zn]/([Zn]+[Sn])%.

AGING EFFECTS ON DYNAMIC PROPERTIES OF PURE METALS: SIMULATING HELIUM BUILDUP THROUGH IMPLANTATION

C.R. Lear, S.J. Fensin
MST-8: Materials Science in Radiation & Dynamics Extremes, Los Alamos National Laboratory
UNCLASSIFIED, LA-UR-20-XXXXX

Prolonged irradiation of metals results in the formation of excess microstructural defects, aging of components, and reduced service life. The accumulation of helium under these conditions is key to the longevity of plasma facing materials in fusion systems and to our confidence in structural materials for fission systems. Unfortunately, the irradiated sample volumes required for traditional, large-scale mechanical testing of high temperature and/or strain rate effects are prohibitive in terms of safety, time, and expense, and thus considerable gaps exist in the available, reliable data for mechanical strength in the presence of helium defects. In this study, a series of Richtmyer-Meshkov Instability (RMI) experiments were carried out on pure metal targets, such that material strength data could be determined solely for helium implanted surface layers.

To investigate the effects of helium concentration, 35 mm diameter Cu targets, shown in Fig. a, were implanted at room temperature to 1000, 2000, and 4000 appm. (Surrogate, electropolished samples of Cu were identically implanted for characterization using electron microscopy.) Targets were subjected to a 1 km/s impact in the 80 mm bore gas-gun in MST-8 at LANL, for peak shock stresses of ~30 GPa. Machined perturbations on the target surfaces were inverted at these high stresses, with valleys in the original pattern growing into "spikes" on impact. The rate of this change was tracked across the target surface using photon Doppler velocimetry (PDV), a high-speed laser interference technique. Trends in the PDV peak velocity, see Fig. b, with perturbation "kh" ($kh = 2\pi h/\lambda$) were compared to hydrocode simulations of shock to estimate the materials strength of implanted and unimplanted surface regions without interference from deeper layers of the target. This analysis revealed no significant increase in flow stress with helium implantation, in keeping with the general independence of instantaneous yield strength from non-dislocation obstacles at high strain rates (~10^7 s^{-1}). However, analysis of the ejecta (i.e., copper particles cast off from the surface during impact) was more intriguing.. Comparison of PDV and piezoelectric probe data indicates that the region implanted to 4000 appm produced a notably finer, faster moving cloud of particles, a sign of possible embrittlement and disintegration of the surface perturbations on impact. This last point is being actively researched, but is consistent with recent molecular dynamics findings.

This work was supported by the U.S. Department of Energy, National Nuclear Security Administration.

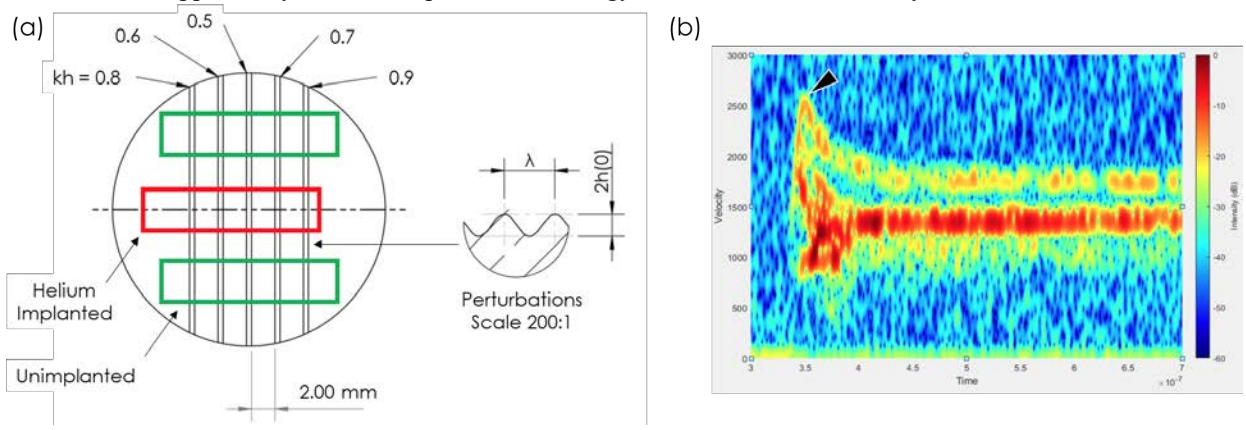

(a) Schematic of 35 mm diameter RMI targets with implanted (red) and unimplanted (green) sample regions. Perturbations are drawn at 200:1 scale vs. scaling of target disk. (b) A velocimetry spectrogram (dB vs. km/s vs. s) recorded for the impact with 1000 appm He implanted target. The peak velocity used to determine materials strength is highlighted with a black arrow.

STUDY OF NOVEL SCANDIUM AND VANADIUM DEFECTS IN DIAMOND FOR QUANTUM SENSING

L.J. Bissell[1], N.W. Gothard[1,2]
[1]Materials and Manufacturing Directorate, Air Force Research Laboratory, Wright-Pattterson Air Force Base, OH [2]Dept. of Chemistry and Physics, Bob Jones University, Greenville, SC

Among defect centers in diamond, the nitrogen-vacancy (NV-) center has shown tremendous potential for application to quantum sensing and information systems [1]. Nevertheless, the NV- site suffers from low conversion efficiency, with considerable non-radiative loss due to the large phonon sideband. Moreover, the 637 nm zero-phonon line is well outside the value of 1550 nm used by telecommunications fiber optics. Given diamond's capacity to host color centers, the potential exists to discover a novel quantum sensor with optical properties suitable for current fiber optics networks among transition metal dopants, due to the additional impurity states such defects introduce. Previous high-throughput, density functional theory (DFT) cluster-based estimates of the absorption energies for transition-metal defects in nanodiamond have identified the scandium-nitrogen (ScN_2) and vanadium-nitrogen (VN) defects in diamond as having potential for infrared emission [2]. Here we attempt to fabricate these defects via ion-beam implantation.

We performed SRIM modeling to determine the implant conditions necessary to implant Sc and N at a depth of ~ 65-68 nm. For each element, 3 doses were made at increasing energies to distribute the dopant profile across the target depth range, and the fluences were chosen to achieve a 1:2 ratio of Sc:N atomic concentration. A similar approach was used to implant VN centers. The ScN_2 implantation was performed at the Michigan Ion Beam Laboratory, and the VN implantation was performed by Leonard Kroko, Inc. The target substrate was an electronic grade chemical vapor deposition diamond from element 6. The substrate was sectioned into 4 implant areas. V fluences of ~ 1 x 10^{11} and ~ 2 x 10^{10} were used in areas 1 and 2, respectively, targeting the creation of single VN centers with an average separation > 0.5 um. Sc fluences of ~ 4 x 10^{9} and ~ 2 x 10^{13} ions/cm^2 were used in areas 3 and 4, respectively. The rationale for these fluences was to create single ScN_2 centers in area 3 and observe an electron paramagnetic resonance (EPR) signature from the centers in area 4.

Following implantation we will perform time resolved photoluminescence (TRPL) to identify optically active defect centers in the visible and infrared, then perform annealing at 1600 C. At this temperature N atoms are mobile [3] and we expect that they will migrate to nearby Sc or V atoms and form ScN_2 or VN centers, respectively. Further characterization will include: 1) observing the effect of the annealing on the centers through TRPL; 2) characterizing the opto-magnetic activity of identified defects centers using optically-detected magnetic resonance; and 3) EPR measurements to determine the structure of the defect centers.

[1] M. W. Doherty, N. B. Manson, P. Delaney, F. Jelezko, J. Wrachtrup, and L. C. L. Hollenberg, "The Nitrogen-Vacancy Colour Centre in Diamond," Physics Reports, **528**, (2013) 1–45.

[2] N.W. Gothard, T. Zhan, R.H. Mattish, C.M. Collins, D.S. Dudis, and L.J. Bissell, "Identification of Novel Split-Vacancy Transition Metal Color Centers in Nanodiamond via Time-Dependent Density Functional Theory," submitted to J. Phys. Chem. Solids

[3] T. Lühmann, N. Raatz, R. John, M. Lesik, J. Rödiger, M. Portail, D. Wildanger, F. Kleißler, K. Nordlund, A. Zaitsev, J.-F. Roch, A. Tallaire, J. Meijer, and S. Pezzagna, "Screening and Engineering of Colour Centres in Diamond," J. Phys. D: Appl. Phys. **51**, 483002.

CANADIAN NUCLEAR LABORATORIES AND ACCELERATED IRRADIATIONS AT MIBL

M. Mattucci
Canadian Nuclear Laboratories (Chalk River Labs), Ontario, Canada

With the decommissioning of the National Research Universal (NRU) reactor at Canadian Nuclear Laboratories, irradiation sources and accessibility to irradiated material has become increasingly important. Accelerated ion irradiations performed at MIBL have been crucial to CNL. These types of irradiations can quickly access the viability of novel materials and provide insight into irradiation damage when material is limited or not accessible. CNL has used accelerated irradiations to examine material degradation in the long term operation of the current fleet of reactors, which help inform larger neutron irradiation programs. These project that have utilized the MIBL are highlighted below.

Access the Effects of Irradiation Temperature in 304L SS to support LTO of CANDU® Reactor

Austenitic stainless steels, namely 304L, 308L and 316L SS, are used widely in the structural components of light water reactors (LWRs). These components are subjected to a reactor operating temperature of ~330°C. In the CANDU® reactor, the heavy water moderator is contained with a Calandria vessel. The Calandria vessel is a large horizontal cylindrical shell, fabricated from welded plate material, with associated end walls/tubesheets and the primary materials of construction are 304L (base) and 308L (weld metal). It is subjected to an operating temperature of 60-80°C. Many of these components were designed with the intent to remain fit for service for the full service life of the reactor. This study was performed to access the effects of irradiation temperature on the microstructure of 304L SS, using 2MeV proton irradiation at 360°C and 100°C [1].

Validating ATF Cladding in Reactor Operating Conditions

Ongoing work at CNL includes access the corrosion properties of FeCrAl alloys and Coated Fuel Claddings. Proton Irradiation was performed on FeCrAl alloys and subsequent autoclave exposures are currently being performed. These results will be compared to a pre-irradiated foil, re-irradiated in the is-situ IAC proton irradiation rig at the MIBL. Oxide morphology will be compared between the in-situ and ex-situ exposure.

[1] C. D. Judge *et al.*, "Microstructural Characterization of Proton Irradiated 304L SS at 100°C and 360°C," in *19th Int'l Conference on Environmental Degradation of Materials in Nuclear Power Systems - Water Reactors*, 2019.

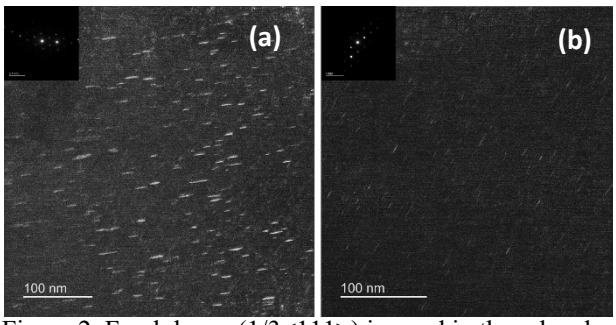

Figure 2. Frank loops (1/3<111>) imaged in the rel-rod condition, for (a) 360°C and (b) 100°C irradiation conditions.[1].

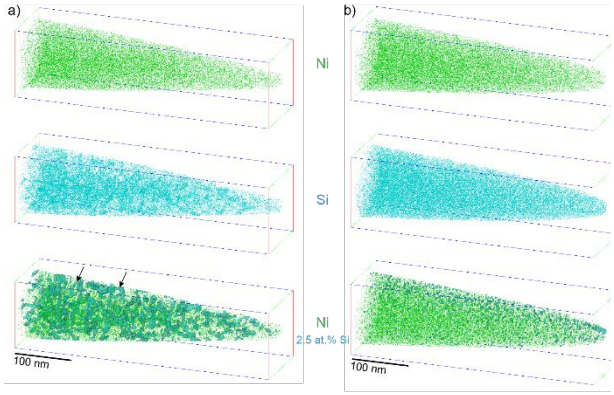

Figure 3. Atom maps of typical APT data from irradiated regions of a) 360°C and b) 100°C samples. Atom maps are shown for Ni, Si (2% and 25% of collected ions displayed for visualization purposes, respectively) and Ni with isosurfaces of 2.5 at.% Si.[1].

EVALUATION ON EFFECTS OF THE THERMAL AGING AND IRRADIATION OF AUSTENITIC STAINLESS STEEL WELDS IN PWRs

B.S. Kong[1], J.H. Shin[1], H.J. Lee[2] and C. Jang[1]
[1]Dept. of Nuclear and Quantum Engineering, Korea Advanced Institute of Science and Technology, Daejeon, Republic of Korea
[2]Central Research Institute, Korea Hydro & Nuclear Power Co., Ltd, Daejeon, Republic of Korea

The austenitic stainless steel welds (ASSWs) are extensively used in primary water piping system and in-core components, such as pressurizer surge-line, weld over-lay cladding and reactor vessel internals in pressurized water reactors (PWRs). The austenitic stainless steel welds are required to contain 5 - 20 vol. % of δ-ferrite in austenite matrix to avoid hot-cracking during welding procedure. Although duplex structure containing certain amount of δ-ferrite have superior strength, corrosion resistance and weldability, it has been recognized that δ-ferrite are significantly susceptible to thermal aging embrittlement after long-term thermal aging at service temperature in PWRs. It was known that δ-ferrite phase breaks down into embrittling phases like Cr-rich (α'), Fe-rich (α) and Ni, Si-rich intermetallic phase because of miscibility gap in the Fe-Cr system. Thus, the mechanical properties like tensile elongation and fracture toughness could be degraded after long-term thermal aging.

The purpose of this study is to investigate thermal aging effect and combined effect on thermal aging and irradiation for austenitic stainless steel weld in PWRs. First of all, the microstructure evolution and mechanical behavior of E308 weld were studied after thermal aging at 400 ℃ up to 20,000 h. The microstructure evolution induced by thermal aging was observed using transmission electron microscope (TEM). The mechanical property changes by thermal aging embrittlement was evaluated various kinds of mechanical testing, such as tensile, fracture toughness, nanopillar compression tests. Furthermore, considering the synergism of thermal aging and neutron irradiation proton irradiation experiment was conducted after thermal aging at 400 °C for 20,000 h. The enhancement of the spinodal decomposition and formation of secondary phases in the δ-ferrite will be observed using TEM. Based on the mechanical property degradation by nanopillar compression tests, hardening behavior among the condition of as-welded, thermally aged and proton irradiated after thermal aging will be investigated in this study.

This study is mainly supported by the Korea Hydro and Nuclear Power Co., Ltd. as the Proactive Material Aging Management Project. Part of the funding is provided as Nuclear R&D Program (2015M2A8A2074798) of the MSIP/NRF of Rep. of Korea.

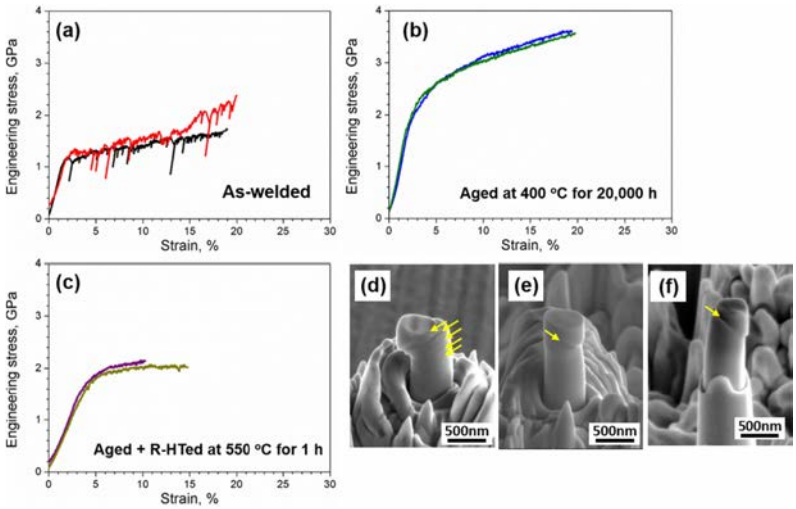

Stress-strain curves of δ-ferrite nanopillar compression tests and SEM micrographs of δ-ferrite nanopillar after compression tests; (a) and (d) as-welded, (b) and (e) aged at 400 °C for 20,000 h, and (c) and (f) aged+ R-heat treated at 550 °C for 1 h.

IRRADIATION ASSISTED STRESS CORROSION CRACKING OF STAINLESS STEEL 304L IN PRIMARY WATER ENVIRONMENT

S. C. Yoo, J. Ham, Y. Lee and J. H. Kim
Department of Nuclear Science and Engineering, Ulsan National Institute of Science of Technology, Republic of Korea

Stainless steel 304L (SS304L) is used in internal structures of nuclear power plants, suffers severe irradiation due to its location near the nuclear fuel. Severe irradiation causes irradiation assisted stress corrosion cracking (IASCC) which leads to cracking or failure of the components made with SS304L. However, IASCC resistance of SS304L was not studied enough due to difficulties in quantitative evaluation of IASCC resistance.

UNIST going to evaluate IASCC initiation resistance of SS304L via slow strain rate test (SSRT) with direct current potential drop (DCPD) system for online crack initiation monitoring. Since it is hard to use neutron irradiated specimen in normal laboratory environment, proton beam radiation was used to simulate the effect of neutron irradiation. Radiation was conducted in Michigan Ion Beam Laboratory (MIBL) with 2.0 MeV (~10^{-5} dpa/sec) proton source for 1, 3and 7 dpa.

Detailed microstructure will be evaluated to investigate the effect of proton irradiation. Dislocation loop and radiation induced segregation are expected to be observed in TEM analysis. Also, IASCC initiation time which will be deduced from SSRT would be accelerated by proton irradiation. It is known that dislocation loops could do a role as crack initiation source for IASCC since those structures are prone to stress concentration. Also, radiation induced segregation make the grain boundary vulnerable to corrosion, which could cause IASCC initiation.

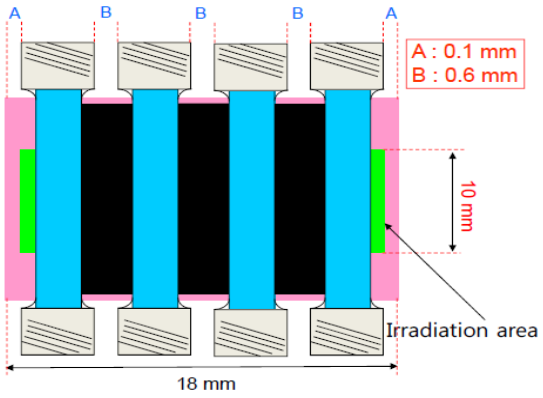

Figure 1. Specimen stage setup for proton irradiation

Figure 2. Specimen mounted in SSR´ facility

PROTON-IRRADIATED STEEL SPECIMENS FOR CALIBRATION OF A CRYSTAL PLASTICITY MODEL

J.-M. Scherer, J. Hure, B. Tanguy
DEN-Service d'Etudes des Matériaux Irradiés, CEA, Université Paris-Saclay,
F-91191, Gif-sur-Yvette, France

In the context of ductile rupture of irradiated face-centered cubic (FCC) materials, the goal of this study is to calibrate a crystal plasticity model through tensile testing of non-irradiated and proton-irradiated AISI 316L single crystal specimens. Pre- and post-irradiation Transmission Electron Microscopy (TEM) observations of the specimens will provide dislocation and Frank dislocation loop densities which are input data of the model. The crystal plasticity model will be calibrated through comparison of the numerical predictions to the experiments.

To perform tensile tests on proton-irradiated AISI 316L single crystal specimens, a 0.9 mm thick single crystal plate of area 18mm x 20mm was irradiated over a 10mm x 18mm area. A single irradiation experiment was conducted using Wolverine beamline #2 with 3MeV H^+ beam. The figure (a) below shows the damage profile, in which a total dose of 1 displacements per atom (dpa) at 15 µm depth was collected with a total fluence of $3.4x10^{19}$ions/cm^2. Specimen temperature was monitored to 350°C which is the temperature for which the defect microstructure is comparable to a neutron irradiation at 300°C typical of Pressurized Water Reactors (PWR). Temperature control was made with thermal imaging calibrated before irradiation with thermocouples spot-welded outside the irradiation area (see figure (b)). Pressure, temperature and beam currents were recorded during the irradiation experiments.

Tensile specimens will be cut in this plate using a wirecut electric discharge machine. In order to perform the tensile tests on an almost homogeneously irradiated layer only (~30 µm thick, see figure (a)), the non-irradiated layer will be removed by mechanical polishing.

a)

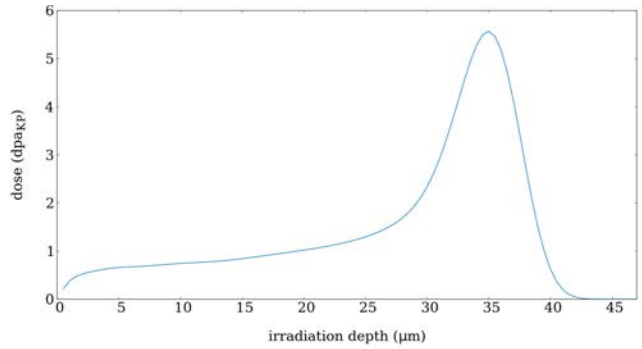

b)

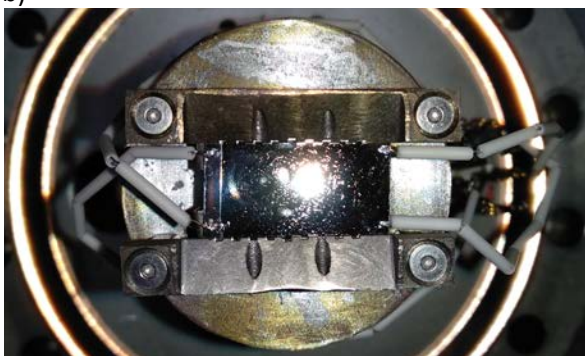

Displacements per atom with respect to distance to specimen surface for 3 MeV H^+ in AISI 316L steel calculated by SRIM (a), and irradiation stage with AISI 316L single crystal plate and welded thermocouples (b).

IRRADIATION-ACCELERATED CORROSION BEHAVIOR OF ITER-GRADE CuCrZr ALLOY

J. J. H. Lim[1], G. Fulton[1], R. Hanbury[2], and G.S. Was[2]
[1]United Kingdom Atomic Energy Authority, UK
[2]Department of Nuclear Engineering & Radiological Sciences, University of Michigan

The simultaneous effects of displacement damage and radiolysis on the corrosion of *ITER-grade CuCrZr* alloy was studied using the unique in-situ proton irradiation-accelerated corrosion facility at the Michigan Ion Beam Laboratory (MIBL). The aim of this study is to understand the effect of irradiation-accelerated corrosion (IAC) of *ITER-grade CuCrZr* alloy under pressurized, de-aerated water condition up to displacement damage of ~0.1dpa and ~0.3dpa and at different water coolant temperature, i.e. ~35°C, ~150°C and ~325°C and. These temperatures correspond to the upper estimate for water coolant temperatures in fusion reactors and ambient beam heating conditions. The outcome of this study will help to determine whether simultaneous displacement damage and radiolysis dictates the effective component lifetime for divertor coolant pipes of Tokamak-type fusion reactor.

Preliminary results indicate that displacement damage has a direct impact on corrosion kinetics. Figure 1 shows that the CuCrZr alloy that exposed to proton irradiation under de-aerated water, i.e. region within the red dotted circle, was fully eroded; whereas, the region that exposed to just de-aerated water, i.e. region within the yellow dotted circle, has a layer of oxidized surface. Further microstructural characterizations will be performed to understand the oxide layer that formed after exposed to irradiation and de-aerated water.

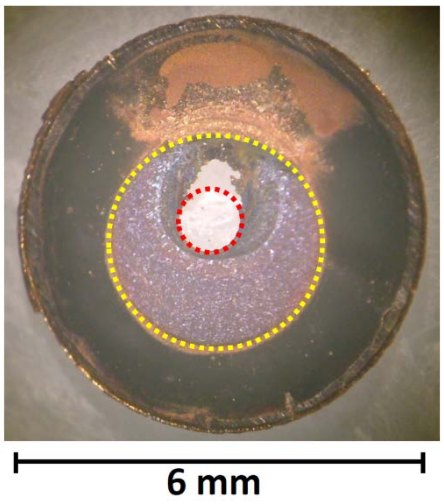

A proton irradiated ITER-grade CuCrZr sample in de-aerated water environment at 150 °C up to 0.3 dpa. The region within the red dotted circle was proton irradiated. The region within the yellow dotted circle was in de-aerated water.

DUAL ION BEAM IRRADIATION TO EMULATE THE HIGH DOSE NEUTRON IRRADIATION ON THERMAL TESTING REACTOR IN AUSTENITIC STAINLESS STEEL

Y. Miyahara[1], S. Taller[2], F. Naab[2], T. Kubley[2], E. Uberseder[2], O. Toader[2], G.S. Was[2]
[1]Central Research Institute of Electric Power Industry, CRIEPI, Yokosuka, Japan
[2] Department of Nuclear Engineering & Radiological Sciences, University of Michigan

A series of neutron irradiation of solution annealed austenitic stainless steels were conducted in past IASCC project executed by JNES. In this JNES IASCC project, neutron irradiation at the Japan Materials Testing Reactor (JMTR) and post irradiation tests such as TEM observation, mechanical properties tests were carried out to the materials irradiated up to about 12 dpa at 288°C. Dual ion beam irradiation can be used as a useful tool to investigate the high dose irradiated materials that can be provide the further understanding of materials degradation due to the neutron irradiation. The objective of this study is to understand the microstructural evolution of austenitic stainless under the high dose irradiated conditions in thermal testing reactor JMTR.

Prior to the high dose irradiation tests, three dual ion irradiation tests were performed to confirm the temperature shift between dual ion beam irradiation and neutron irradiation by comparing the corresponding microstructure.

The archive material of solution annealed type 316L stainless steel used in JNES IASCC project was used for dual ion beam irradiation tests. Samples were fabricated using electrical discharging machine in the shape of bars with a dimensions of 3 mm x 1.5 mm x 20 mm. The surface of bar samples was mechanically polished then finished by electropolishing.

Dual ion beam irradiations were conducted using the 3 MV Pelletron accelerator “Wolverine” and the 1.7 MV Tandem accelerator “Maize” with 5 MeV Fe^{++} and 2.85 MeV He^{++} ion beams. Dual ion beam irradiation conditions were summarized in table below including JMTR irradiation conditions for comparison. The dose of Fe^{++} in table is correspond to the damage at 600 nm depth. Dual ion beam irradiation temperature of 340°C was estimated from the Mansur’s relation to reproduce the microstructure such as dislocation loops. The figure below shows the example of samples mounting on the irradiation stage of dual ion beam irradiation. Two samples for each irradiation condition was placed between the reference samples made of same material. Four thermocouples were welded on to the reference samples to calibrate the six points of infrared temperature measurement on the sample irradiated area in 6 mm x 6 mm. The samples temperature during irradiation was controlled by the average temperature of infrared temperature measurements.

Facility	Temperature (°C)	Dose rate (dpa/s)	Dose (dpa)	He/dpa ratio (appm He /dpa)
JMTR	288	2.5×10^{-7}	1.5 /neutron	~2
MIBL	340	8.0×10^{-4}	1.5 /Fe^{++}	2.0
JMTR	288	2.5×10^{-7}	4.4 /neutron	~2
MIBL	340	8.0×10^{-4}	4.4 /Fe^{++}	2.0
JMTR	288	2.5×10^{-7}	12.4 /neutron	~2
MIBL	340	8.0×10^{-4}	12.4 /Fe^{++}	2.0

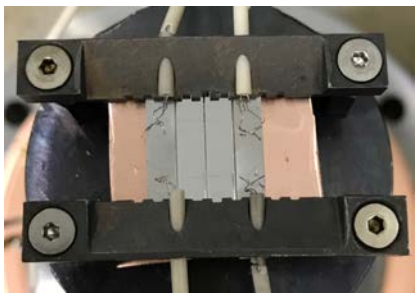

Irradiation conditions (left) and samples setting for dual ion beam irradiation (right).

DEUTERON IRRADIATION OF A ^{12}C AND ^{13}C TARGETS AS A NEUTRON SOURCE FOR ACCELERATOR-BASED BORON NEUTRON CAPTURE THERAPY (AB-BNCT)

A.A. Bertolo[1,2], M.F. del Grosso[2,3], F.D. Becchetti[4], T. Kubley[5], O. Toader[5], G.S. Was[5]
1. Sabato Institute, National University of San Martin, Argentine , 2. National Atomic Energy Commission, Argentine, 3. National Scientific and Technical Research Council, Argentine, 4. Physics Department, University of Michigan, United States, 5. Nuclear Engineering and Radiological Sciences, University of Michigan, United States

Accelerator Based Boron Neutron Capture Therapy (AB-BNCT) is a cancer treatment therapy that is being developed worldwide and also in Argentina. The use of accelerators could allow to obtain a neutron beam with a suitable energy and fluence, which is a fundamental requirement to perform the therapy. Accelerators are much easier to turn off than reactors, and they do not have a permanent inventory of radioactive materials; they are less costly and complex and much easier to license from the radioprotection point of view. Accelerators can be installed in hospitals, in contrast to nuclear reactors which have been used so far to perform BNCT.

Neutron production targets suitable for AB-BNCT are being studied around the world, in particular in Argentina as a part of the project to develop accelerators for BNCT and other applications. Under operation these targets will be exposed to different extreme conditions created by the impinging of a high intensity beam. The target assembly should have the ability to drain a power density of up to 1 kW/cm^2 and withstand the radiation and hydrogen damage induced by the beam.

Materials like beryllium, liquid lithium and carbon were considered as possible candidates for the neutron production target and several nuclear reactions have been studied for their application on BNCT. The $^{13}C(d,n)^{14}N$ reaction turns out to be one of the best for AB-BNCT because of beneficial materials properties inherent to carbon and its relatively large neutron production cross section. In fact, both $^{12}C(d,n)$ and $^{13}C(d,n)$ reactions are very prolific, especially in the forward direction where the neutron yield is comparable to that generated by the beryllium. The power dissipation from these targets does not demand a sophisticated cooling system, but simply the heat is exchanged by radiation with the water-cooled vacuum chamber wall. Unfortunately, nuclear production targets made of ^{13}C are not commercially available. In that sense, a ^{12}C and ^{13}C targets are currently being developed at the National Atomic Energy Commission, Argentine (CNEA), this represents a major challenge from the point of view of physics and materials engineering, because the target will be subjected to intense thermomechanical stresses, as well as damage by hydrogen and radiation induced by direct impact of the deuteron beam.

In this work, samples made of ^{12}C and ^{13}C, were irradiated at the Wolverine accelerator in the Michigan Ion Beam Laboratory (MIBL). In this case, ^{12}C and ^{13}C enriched samples were directly irradiated by a deuteron beam of 1.5, 3 and 6 MeV, without any additional shielding. Neutron measurements were carried out with deuterated (^2H-based) organic scintillators, unlike conventional ^1H-based scintillators can generate pulse-shape gated neutron energy spectra 1 to 30 MeV without need for time-of-flight (ToF). Encouraging results were obtained after deuteron irradiations, as can be seen in the pulse-shape discrimination (PSD) of the 6 MeV deuteron irradiations of ^{12}C and ^{13}C targets.

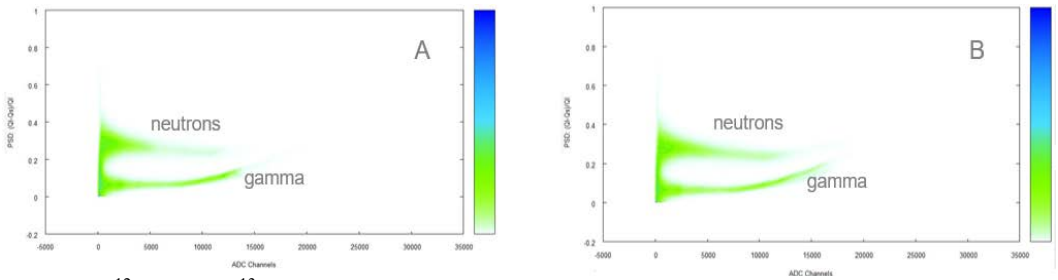

PSD spectra for (a) ^{12}C and (b) ^{13}C targets irradiated with a 6 MeV deuteron beam.

Teaching

NERS 425 LABORTORY ON NUCLEAR REACTION ANALYSIS

M. Atzmon, F. Naab and O. Toader
Department of Nuclear Engineering and Radiological Sciences, University of Michigan

For one of the modules in the NERS 425 course, students conducted an experiment to determine the stoichiometry of a Ti_xN_y sample using the reaction between a deuterium particle and a nitrogen nucleus: $N^{14}(d,\alpha)C^{12}$. Nuclear reaction analysis (NRA) is a well-established surface analysis technique. In this method, an energetic particle (deuterium – produced by the Tandem accelerator at MIBL) interacts with the nucleus of an N atom in the target to give a reaction product (α particle) that can be measured. The students also use the backscattered yield from an RBS experiment to determine the amount of Ti in the sample by implementing simulation codes like RUMP or SIMNRA with the given experimental spectrum.

In the first meeting, prior to the experiment, a short tutorial was given to the students on the accelerator, electronics, detectors, software, and vacuum components. After that, they worked independently with just the basic support from the MIBL staff (required in the setup of the ion beam and the collection of the spectra). The students decided on a few parameters of the experiment (beam energy, time for spectrum acquisition, etc.), and obtained spectra similar to the ones in the figure.

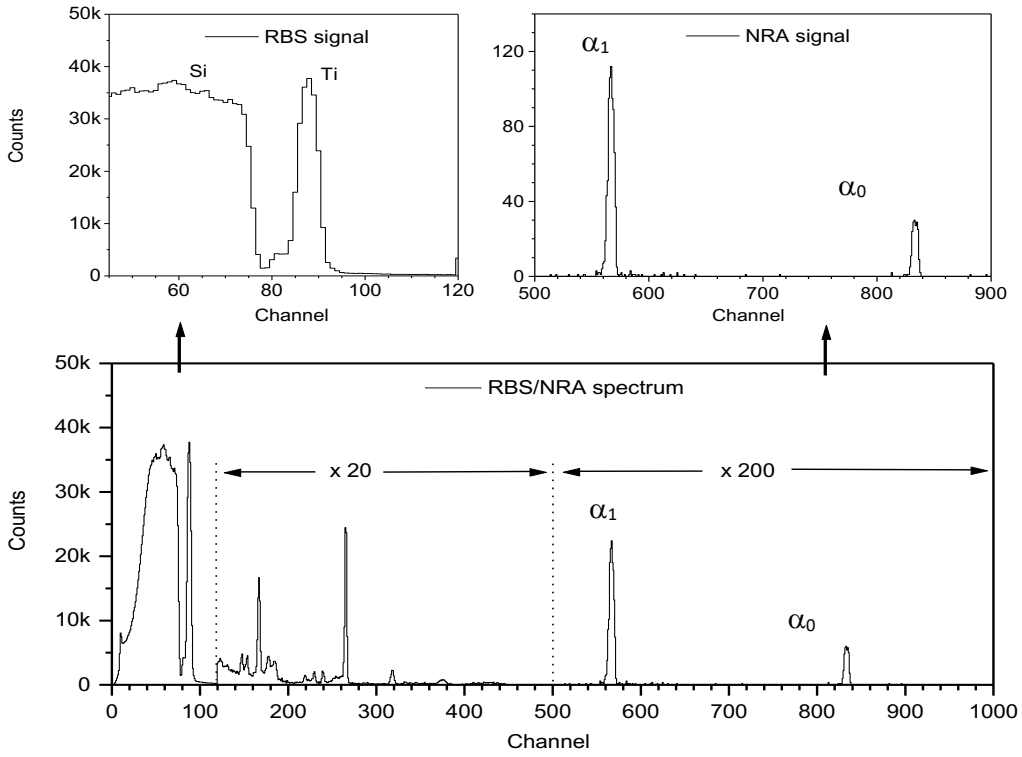

Typical RBS/NRA spectrum for the TiN film obtained during class. Conditions: beam energy: 1.4 MeV D^+, solid angle 5 msr., detector angle 150°.

PUBLICATIONS AND PRESENTATIONS

Publications

1. B. Khur, D. Farkas, I. M. Robertson, D. Johnson, G. Was, "Stress Localization Resulting from Grain Boundary Dislocation Interactions in Relaxed and Defective Grain Boundaries," Metall. Mater. Trans. A. 51 (2020) 667-683.

2. C. Ye, J. Xue, T. Liu, R.Shu, Y. Yan, Y Liao, Q. Ren, G. Ran, K. Sun, L. Jiang, P. Xiu, L. Wang, "The Microstructure Evolution in a SiCf/SiC composite under Triple Ion Beam Irradiation," Ceramics Int'l. 46 (2020) 9901.

3. G. S. Was, D. Petti, S. Ukai, S. Zinkle, "Materials for Future Nuclear Energy Systems," J. Nucl. Mater. 527 (2019) 151837.

4. M. Wang, M. Song, G. S. Was, J. L. Nelson, "The Roles of Thermal Mechanical Treatment and Phase in the Stress Corrosion Cracking of Alloy 718 in Primary Water," Corr. Sci. 160 (2019) 108168.

5. R. E. Stoller, M. B. Toloczko, G. S. Was, A. G. Certain, S. Dwaraknath, F. A. Garner, Erratum to "On the use of SRIM for Computing Radiation Damage Exposure" [Nucl. Instrum. Methods Phys. Res. B 310 (2013) 75-80], Nucl. Instrum. Methods Phys. Res. B 459 (2019) 196-197.

6. S. Taller, Z. Jiao, K. Field, G. S. Was, "Emulation of Fast Reactor Irradiated T91 using Dual Ion Beam Irradiation," J. Nucl. Mater. 527 (2019) 151831.

7. R. D. Hanbury, G. S. Was, "Oxide Growth and Dissolution on 316L Stainless Steel during Irradiation in High Temperature Water," Corr. Sci. 157 (2019) 305-311.

8. M. Reyes, P. Wang, G. Was, J. Marian, "Determination of Dose Rate Effects on Zircaloy Oxidation Using Proton Irradiation and Oxygen Transport Modeling," J. Nucl. Mater. 523 (2019) 56-65.

9. D. C. Johnson, B. Kuhr, D. Farkas, G. S. Was, "Quantitative Linkage between the Stress at Dislocation Channel- Grain Boundary Interaction Sites and Irradiation Assisted Stress Corrosion Cracking," Acta Mater. 170 (2019) 166-175.

10. P. L. Andresen, G. S. Was, "A Historical Perspective on Understanding IASCC," J. Nucl. Mater. 517 (2019) 380-392. **Invited Review**

11. C. Lear, M. Wang, G. S. Was, "Dual Ion Irradiation of Commercial and Advanced Alloys: Evaluating Microstructural Resistance for High Dose Core Internals," J. Nucl. Mater. 516 (2019) 125-134.

12. B. Heidrich, S. M. Pimblott, G. S. Was, S. Zinkle, "Roadmap for the Application of Ion Beam Technologies to the Challenges of Nuclear Energy Technologies," Nucl. Instr. Meth. Phys. B 441 (2019) 41-45.

13. M. Wang, M. Song, C. R. Lear, G. S. Was, "Irradiation Assisted Stress Corrosion Cracking of Commercial and Advanced Alloys for Light Water Reactor Core Internals," J. Nucl. Mater. 515 (2019) 52-70.

14. M. Song, M. Wang, X. Lou, R. Rebak, G. S. Was, "Radiation Damage and Irradiation-Assisted Stress Corrosion Cracking of Additively Manufactured 316L Stainless Steels," J. Nucl. Mater. 513 (2019) 33-44.

15. T. Kubley, F. Naab, O. Toader, G. Was, "Creation of a remotely monitored and controlled ion beam laboratory using novel hardware and software tools," Nucl. Instr. Meth. Phys. B 438 (2019) 31-37.

Presentations

1. F. U. Naab, O. F. Toader, T. Kubley, G. S. Was, "M. Wang, M. Song, G. S. Was, "Application of the $^{12}C(d,p_0)^{13}C$ nuclear reaction to assess carbon contamination of Fe-Cr alloy samples during ion irradiation," Proc. Ion Beam Analysis Conference, Antibes, France, October 2019.

2. K. Thomas, Z. Jiao, G. S. Was, "Effect of Heavy Ion Irradiation on a' Precipitate Stability in Fe-15Cr," Materials in Nuclear Energy Systems (MiNES) Conference, Baltimore, October 2019.

3. P. Wang, J. Bowman, A,. Motta, G. S. Was "Microstructure Characterization of Proton Irradiated Zircaloy-4," Materials in Nuclear Energy Systems (MiNES) Conference, Baltimore, October 2019.

4. M. Song, K. G. Field, J. T. Busby, C. Topbasi, G. S. Was, "Re-irradiation of Flux Thimple Tubes Using Heavy Ions," Materials in Nuclear Energy Systems (MiNES) Conference, Baltimore, October 2019.

5. S. M. Levine, Z. Jiao, G. S. Was, C. M. Parish, "Re-irradiation of Neutron Irradiaed 304L Stainless Steel to High Damage Levels," Materials in Nuclear Energy Systems (MiNES) Conference, Baltimore, October 2019.

6. S. Taller, Z. Jiao, G. S. Was, "The Role of High Damage Rates on Cavity Nucleation with Co-injected Helium in Dual Ion Irradiated T91 Steel," Materials in Nuclear Energy Systems (MiNES) Conference, Baltimore, October 2019.

7. D. Woodley, Z. Jiao, K. Sun, G. S. Was, "Effect of Helium on Swelling and Bubble and Cavity Evoution in Dual Ion Iradiated HT9 Steel," Materials in Nuclear Energy Systems (MiNES) Conference, Baltimore, October 2019.

8. C. R. Lear, M. Song, M. Wang, G. S. Was, "Dual Ion Irradiation of Commercial and Advanced Structural Materials: High Dose Resistance for Extended LWR Operation," Materials in Nuclear Energy Systems (MiNES) Conference, Baltimore, October 2019.

9. Z. Jiao, J. Hesterberg, G. S. Was, "Comparison of Post-irradiation Annealing Effects in Proton-irradiated and Neutron-irradiated 304 Stainless Steel," Materials in Nuclear Energy Systems (MiNES) Conference, Baltimore, October 2019.

10. G. VanCoevering, B. D. Wirth, G. S. Was, "Helium and Damage Rate Dependence of Swelling in Simulated Ferritic Alloys Using a Hybrid Cluster Dynamics Model," Materials in Nuclear Energy Systems (MiNES) Conference, Baltimore, October 2019.

11. Z. Li, W. Zhong, G. S. Was, B. J. Heuser, "Irradiation Assisted Stress Corrosion Cracking in SA508-304 Weldment Under BWR/NWC Simulated Environment," Materials in Nuclear Energy Systems (MiNES) Conference, Baltimore, October 2019.

12. D. Johnson, M. R. He, I. M. Robertson, D. Farkas, G. S. Was, "Quantification of Local Stress Fields in Crack Initiation in Irradiated Austenitic Stainless Steels," Materials in Nuclear Energy Systems (MiNES) Conference, Baltimore, October 2019.

13. G. S. Was, "The Importance of Conducting Experiments in Reactor-Like Environments for Materials Performance and Development without the Reactor," Materials in Nuclear Energy Systems – MiNES, Baltimore, October 2019. ***Plenary talk***.

14. G. S. Was, "Advanced Materials for Nuclear Energy Applications," 2nd International Conference on Materials Science & Nanotechnology, London, July 2019, *Keynote talk*.

15. G. S. Was, "Synergy between He and H in the Evolution of Cavities in Fusion Blanket Materials," 6th Fusion Materials Technology Cooperation Program Workshop on Theory and Modelling of Nuclear Fusion Materials, Walla Walla, WA, June 2019.

16. G. S. Was, "Mechanisms Behind Irradiation Assisted Stress Corrosion Cracking," Symposium on Environmentally Assisted Cracking: Theory and Practice, Annual TMS Meeting, San Antonio, March 2019.

17. G. S. Was, "Environmental Cracking of Laser-fused Alloys under Non-irradiated and Irradiated Conditions," Symposium on Environmentally Assisted Cracking: Theory and Practice, Annual TMS Meeting, San Antonio, March 2019.

18. G. S. Was, "Accident Tolerant Fuels – Corrosion Behavior, Irradiation Performance and Corrosion under Irradiation," ZIRAT23, Clearwater Beach, FL, February 2019.